Report No. FAA-RD-76-65

(12)

EVALUATION OF NONLINEAR RESILIENT MODULI OF UNBOUND GRANULAR MATERIALS FROM ACCELERATED TRAFFIC TEST DATA

Yu T. Chou

U. S. Army Engineer Waterways Experiment Station
Soils and Pavements Laboratory
P. O. Box 631, Vicksburg, Miss. 39180

AUGUST 1976
FINAL REPORT

Prepared for

DEPARTMENT OF DEFENSE
DEPARTMENT OF THE ARMY
Office, Chief of Engineers
Washington D. C. 20314

U.S. DEPARTMENT OF TRANSPORTATION
FEDERAL AVIATION ADMINISTRATION
Systems Research & Development Service
Washington, D. C. 20591

NOTICES

This document is disseminated under the sponsorship of the Department of Transportation in the interest of information exchange. The United States Government assumes no liability for its contents or use thereof.

The United States Government does not endorse products or manufacturers. Trade or manufacturers' names appear herein solely because they are considered essential to the object of this report.

Technical Report Documentation Page

1. Report No.	2. Government Accession No.	3. Recipient's Catalog No.
FAA-RD-76-65		

4. Title and Subtitle	5. Report Date	6. Performing Organization Code
EVALUATION OF NONLINEAR RESILIENT MODULI OF UNBOUND GRANULAR MATERIALS FROM ACCELERATED TRAFFIC TEST DATA	August 1976	

7. Author(s)	8. Performing Organization Report No.
Yu T. Chou	

9. Performing Organization Name and Address	10. Work Unit No. (TRAIS)
U. S. Army Engineer Waterways Experiment Station Soils and Pavements Laboratory P. O. Box 631, Vicksburg, Miss. 39180	11. Contract or Grant No. DOT-FA73WAI-377

12. Sponsoring Agency Name and Address	13. Type of Report and Period Covered
Federal Aviation Administration and Office, Chief of Engineers, U. S. Army Washington, D. C.	Final Report
	14. Sponsoring Agency Code ARD-430

15. Supplementary Notes

16. Abstract

A method for evaluating the resilient moduli of unbound granular materials is presented herein. The moduli were back-calculated from correlations of performance data of numerous full-scale accelerated traffic test pavements with computed critical stresses and strains of test pavements. The test pavements consisted of conventional flexible pavements as well as all-bituminous concrete (ABC) pavements. The loadings include single and multiple wheels. The stresses and strains in the pavement structures were computed by the finite element technique incorporated with the tried nonlinear stress-strain relations of pavement materials. A general discussion on the nonlinear characteristics of pavement materials and limitations of the finite element computer program is presented. The parameters used to establish the correlations included (a) radial tensile strains at the bottom of the ABC, (b) maximum radial tensile strains and minimum ratios of radial tensile stress to vertical stress in the unbound granular layers, and (c) vertical strains at the subgrade surface. Parameter b was developed only for single-wheel loads. The principle of superposition was used in the computations for multiple-wheel load assemblies. In Appendix A, stresses and deflections computed by the nonlinear-finite element method as compared with actual measurements of stress and deflection for a full-scale flexible test pavement are given. The nonlinear resilient moduli used in the computations were evaluated from traffic test data presented in this report. The nonlinear characteristics of pavement materials under loads are discussed. It is recommended that the nonlinear resilient moduli presented in the report be used to compute pavement responses when laboratory repeated load test data on granular materials are not available.

17. Key Words		18. Distribution Statement
Finite element method Flexible pavements Granular materials	Resilience Stress-strain relations Traffic tests	Document is available to the public through the National Technical Information Service, Springfield, Va. 22151

19. Security Classif. (of this report)	20. Security Classif. (of this page)	21. No. of Pages	22. Price
Unclassified	Unclassified	61	

Form DOT F 1700.7 (8-72) Reproduction of completed page authorized

PREFACE

This report was prepared by the U. S. Army Engineer Waterways Experiment Station (WES), Vicksburg, Mississippi, for the Material Behavior Model Study under the project "New Pavement Design Methodology," sponsored by the Federal Aviation Administration (FAA), U. S. Department of Transportation, under Inter-Agency Agreement DOT FA73WAI-377 (FAA ER-430-002b), and by the Office, Chief of Engineers, U. S. Army (OCE), under RDT&E Project AT04, "Pavements, Soils, and Foundations," Task 02, Work Unit 002, "Material Characterization Procedures." Technical monitor for OCE was Mr. A. F. Muller and for the FAA was Mr. Hisao Tomita.

The study was conducted under the general supervision of Mr. James P. Sale, Chief, Soils and Pavements Laboratory. This report was prepared by Dr. Yu T. Chou.

Directors of WES during the conduct of the investigation and the preparation and publication of this report were BG E. D. Peixotto, CE, COL G. H. Hilt, CE, and COL John L. Cannon. Technical Director was Mr. F. R. Brown.

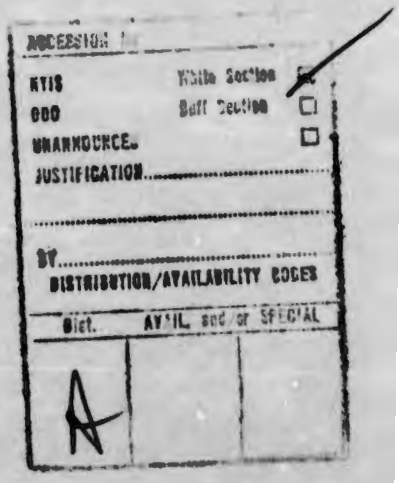

TABLE OF CONTENTS

METRIC CONVERSION FACTORS

Approximate Conversions to Metric Measures

Symbol	When You Know	Multiply by	To Find	Symbol
		LENGTH		
	inches	* 2.5	centimeters	
	feet	30	centimeters	
	yards	0.9	meters	
	miles	1.6	kilometers	
		AREA		
	square inches	6.5	square centimeters	
	square feet	0.09	square meters	
	square yards	0.8	square meters	
	square miles	2.6	square kilometers	
	acres	0.4	hectares	
		MASS (weight)		
	ounces	28	grams	
	pounds	0.45	kilograms	
	short tons (2000 lb)	0.9	tonnes	
		VOLUME		
	teaspoons	5	milliliters	
	tablespoons	15	milliliters	
	fluid ounces	30	milliliters	
	cups	0.24	liters	
	pints	0.47	liters	
	quarts	0.95	liters	
	gallons	3.8	liters	
	cubic feet	0.03	cubic meters	
	cubic yards	0.76	cubic meters	
		TEMPERATURE (exact)		
°F	Fahrenheit temperature	5/9 (after subtracting 32)	Celsius temperature	°C

* 1 in. = 2.54 (exactly). For other exact conversions and more detailed tables, see NBS Misc. Publ. 286, Units of Weights and Measures, Price $2.25, SD Catalog No. C13.10:286.

Approximate Conversions from Metric Measures

Symbol	When You Know	Multiply by	To Find	Symbol
		LENGTH		
	millimeters	0.04	inches	
	centimeters	0.4	inches	
	meters	3.3	feet	
	meters	1.1	yards	
	kilometers	0.6	miles	
		AREA		
	square centimeters	0.16	square inches	
	square meters	1.2	square yards	
	square kilometers	0.4	square miles	
	hectares (10,000 m^2)	2.5	acres	
		MASS (weight)		
	grams	0.035	ounces	
	kilograms	2.2	pounds	
	tonnes (1000 kg)	1.1	short tons	
		VOLUME		
	milliliters	0.03	fluid ounces	
	liters	2.1	pints	
	liters	1.06	quarts	
	liters	0.26	gallons	
	cubic meters	35	cubic feet	
	cubic meters	1.3	cubic yards	
		TEMPERATURE (exact)		
°C	Celsius temperature	9/5 (then add 32)	Fahrenheit temperature	°F

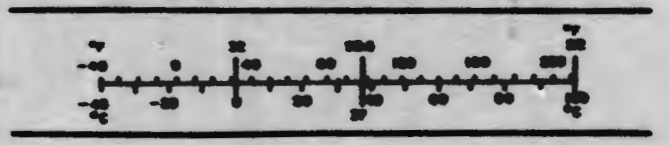

NOTATION

A_0, A_1, A_2, A_3	Material constants
C and ϕ	Mohr-Coulomb strength parameters
E	Dynamic modulus of elasticity
$\|E^*\|$	Complex modulus (Kingham and Kallas[4])
E_i	Initial tangent modulus from the $(\sigma_1 - \sigma_3) \sim \varepsilon$ curve
E_t	Tangent modulus
i	Layer number
$K_1, K_2, K_3, K_4, K_5, K_6$	Material constants
M_R	Resilient modulus
R_f	Ratio of the principal stress difference at failure $(\sigma_1 - \sigma_3)_f$ to the ultimate principal stress difference $(\sigma_1 - \sigma_3)_{ult}$ in the $(\sigma_1 - \sigma_3) \sim \varepsilon$ curve
W	Vertical displacement
γ_{max}	Maximum shearing strain
ε_r	Radial tensile strain
ε_v	Vertical strain
$\varepsilon_z, \varepsilon_r, \varepsilon_\theta$	Strain components in the z, r, and θ directions, respectively
θ	Sum of principal stresses
ν	Poisson's ratio
σ_3	Confining pressure
$\sigma_1, \sigma_2, \sigma_3$	Major, intermediate, and minor principal stresses, respectively
$(\sigma_1 - \sigma_3)_f$	Principal stress difference at failure
$(\sigma_1 - \sigma_3)_{ult}$	Ultimate principal stress difference at failure in $(\sigma_1 - \sigma_3) \sim \varepsilon$ curve
σ_d	Deviator stress $(\sigma_1 - \sigma_3)$
$\sigma_z, \sigma_r, \sigma_\theta$	Stress components in the z, r, and θ directions, respectively

INTRODUCTION

BACKGROUND

For many years, pavement engineers have devoted considerable effort toward improving pavement design methodologies. With the advent of electronic computers, layered analysis has become an essential part of design procedures to evaluate the response of pavement structures to traffic loads. In addition to many other factors, the success of the application of layered analysis to pavement design depends heavily on the proper selection of material properties in each component layer of the pavement. A number of investigators[1,2] have studied the resilient response of granular materials to loads, and they agree that this response is distinctly nonlinear and that stress-deformation characteristics under repeated loads depend greatly on the stress level to which the granular materials are subjected. It has become clear, however, that the resilient moduli of granular materials can be determined only by carefully controlled laboratory tests.

For many years, the Corps of Engineers (CE) has conducted series of full-scale accelerated traffic tests on many different types of pavements under many different types of loads. The majority of the pavements have thick layers of granular materials. The U. S. Army Engineer Waterways Experiment Station (WES) is currently involved in the development of pavement design methodology for the Office, Chief of Engineers, and the Federal Aviation Administration (FAA) which would better utilize the mechanical properties of pavement materials. Efforts have been concentrated to develop laboratory test procedures and techniques to evaluate the resilient and plastic properties of granular materials. Laboratory repeated load tests have been conducted to define the properties of two granular materials which were used recently in the accelerated traffic tests conducted at WES. Since it is both time-consuming and costly to conduct laboratory repeated load tests, it is the purpose of this study to evaluate the resilient moduli of unbound granular materials from the accelerated traffic test data. The moduli so determined should be representative of the average granular materials used by the CE and FAA,

or those materials satisfying CE standard flexible pavement design and construction procedures. Because the test data were collected on many types of pavements at different locations during different periods of time, and the granualr materials in each test pavement possessed different properties, the moduli can be used to compute pavement responses when laboratory repeated load data on granular materials are not available.

OBJECTIVE AND SCOPE

The objective of this study was to develop a procedure to evaluate the resilient moduli of unbound granular materials from the existing accelerated traffic test data. The resilient modulus is the repeated axial stress in triaxial compression divided by the recoverable axial strain. The moduli so determined would represent the average granular materials used by the CE and FAA.

The test pavements for which data were used included conventional flexible pavements and all-bituminous concrete (ABC) pavements. Both single- and multiple-wheel loadings were employed. The stresses and strains in the pavement structures were computed by the nonlinear finite element method. For asphaltic concrete (AC) surfaces, the moduli were determined based on the measured average pavement temperature during the traffic period. For unbound granular materials, the following nonlinear model was used

$$M_R = K_1 \theta^{K_2} \qquad (1)$$

where

M_R = resilient modulus

K_1, K_2 = material constants

θ = sum of principal stresses

For cohesive subgrade soils, the relation $E = 1500\ CBR$ where E is the dynamic modulus of elasticity and CBR is the California Bearing Ratio was used to determine the modulus from the measured CBR values. The constants K_1 and K_2 were evaluated from the established

correlations between computed parameters and the observed performance. The computed parameters are:

a. Radial tensile strains at the bottom of the AC layers.

b. Maximum radial tensile strains and minimum ratios of radial tensile stress to vertical stress in the unbound granular layers.

c. Vertical strains at the subgrade surface.

Parameter b was developed only for single-wheel loads. The principle of superposition was used in the computations for multiple-wheel load assemblies.

The salient features of the established correlations are discussed in this report. The measured stresses and deflections obtained from one of the multiple-wheel heavy gear load test sections and the values computed by the finite element method are compared, and the nonlinearity of materials is discussed. The nonlinear moduli used in the computations were evaluated from traffic test data presented in this report.

THEORETICAL COMPUTATIONS

To compute the stresses and strains in a pavement structure under loads, the commonly used methods are Boussinesq's homogeneous linear elastic analysis, Burmister's linear elastic layered analysis, and the nonlinear finite element method. The first and second methods have been used extensively; their acceptance is probably mainly due to their simplicity rather than their accuracy. A study conducted at the U. S. Army Engineer Waterways Experiment Station (WES)[3] on the use of these two theories had the following conclusions:

a. The measured vertical stresses were generally in excess of those computed from the linear layered analysis; the measured vertical stresses along the load axis of a single wheel were in fairly good agreement with those predicted by the homogeneous analysis of Boussinesq.

b. Comparisons of the computed and measured deflections at various depths indicated that both the homogeneous and the linear layered analysis are quite inadequate.

c. The shapes of the theoretical and measured stress and deflection basins were distinctly different. The measured stress and deflection basins appeared to be more confined to the vicinity of the tire than was indicated by the linear analysis. For both stresses and deflections, the Boussinesq solution gave results closer to the measurements than those given by the linear layered analysis.

Based on the results using these two analyses, the third method, nonlinear finite element analysis, incorporated with nonlinear soil characterizations, seems to be the most powerful tool in pavement analysis and research.

For this study, the nonlinear moduli of granular materials were back-calculated from correlations of performance data of numerous full-scale accelerated traffic test pavements with computed critical stresses and strains of test pavements. A finite element program was used in the computations. With the evaluated nonlinear moduli, the stresses and deflections computed for one of the multiple-wheel heavy gear load test sections were compared with values measured by instrumentation which was embedded in the sections. The results are presented in Appendix A. Good agreement was obtained between measured and computed results. For

ABC test pavements, computer programs based on Burmister's linear layered elastic analysis were used, with the AC divided into layers according to the temperature variations. The use of Burmister's theory was justified since the strength of AC depends on temperature but not on the stress level. As will be explained later in the report, since a constant modulus was used for subgrade soils for all test pavements, the use of the linear layered theory for ABC pavements is justified.

CONCEPT

The purpose of this study is to evaluate the resilient moduli of the unbound granular materials from the accelerated traffic test data. The procedure involved is actually a back-calculation from the observed response of the pavement system, i.e., the measured performance and instrumentation data. The rationale behind this approach is based on the following two hypotheses:

a. When the correct stress-strain relations of pavement materials are known or properly simulated, the computed stresses and deflections should compare favorably with the values actually measured from the field test sections.

b. Definite correlations exist between pavement response to the loads and the performance of the pavements. When correct stress-strain relations of pavement materials are properly selected, the pavement responses can be computed by the nonlinear finite element method and the correlations can be established. Therefore, the closer the representation of material properties, the better the correlations will be.

The detailed description for evaluating the moduli of granular materials is presented later in the report.

FINITE ELEMENT ANALYSIS

The nonlinear finite element program used in this study was obtained from the University of California at Berkeley. The program is suitable only for analysis of axisymmetric solids. The pavement structure is first idealized as an assemblage of a finite number of discrete structural elements interconnected at a finite number of joints or nodal points. The sizes of the elements are chosen to vary in accordance with the anticipated stress gradients. The elements are actually complete

rings in the horizontal direction, and the nodal points are circular lines in plane view. There is a boundary on which the nodal points are fixed and a vertical boundary on which the nodal points are constrained from moving radially. The meshes used in this study are shown in Figure A1.

The surface circular load is assumed to be applied in steps so that the nonlinear stress-strain behavior and the modulus-stress dependency of the material can be included in the analysis. Therefore, the accuracy of the solution is a function of the number of load increments used, with greater accuracy being associated with smaller load increments. Also, the accuracy can be improved by increasing the number of elements into which the pavement structure is divided. In this study, ten load increments were generally used.

It should be noted that the nonlinear finite element program used in this study employs many idealized assumptions which are unrealistic for real pavements. The most critical assumption is discussed in the following paragraphs.

Of the many unrealistic assumptions involved in the finite element method, the assumption of continuous contact between each interface seems to be most serious. According to the linear theory of elasticity, the relations of stress and strain components along each interface are:

$$\sigma_{z_i} = \sigma_{z_{i+1}}, \quad \sigma_{r_i} \neq \sigma_{r_{i+1}}, \quad \sigma_{\theta_i} \neq \sigma_{\theta_{i+1}}, \quad \varepsilon_{z_i} \neq \varepsilon_{z_{i+1}},$$

$$\varepsilon_{r_i} = \varepsilon_{r_{i+1}}, \quad \varepsilon_{\theta_i} = \varepsilon_{\theta_{i+1}}, \quad \gamma_{max_i} \neq \gamma_{max_{i+1}}, \quad W_i = W_{i+1} \qquad (2)$$

where

σ_z , σ_r , σ_θ = stress components in the z , r , and θ directions

ε_z , ε_r , ε_θ = strain components in the z , r , and θ directions

i = layer number

γ_{max} = maximum shearing strain

W = vertical displacement

Although Equation 2 is for the linear theory of elasticity, it also holds true for the piece-wise nonlinear theory used in this study.

Under rolling tire loads, both vertical and horizontal loads are applied to the pavement. It is conceivable then that slip could occur along each interface, particularly during braking operations. The assumption of the continuity of radial and tangential strain components along each interface is apparently incorrect. Some computer programs are now capable of considering slippage along interfaces, but the degree of slippage in real pavement structures may be difficult to determine.

MATERIAL CHARACTERISTICS

The test pavements analyzed in this study consisted of conventional flexible pavements (i.e., AC surface courses and unbound bases), ABC pavements, and pavements with stabilized layers. Since pavement materials are subjected to repetitive applications of traffic loads and since the stress intensity in pavements is generally small (well below the failure strength of the materials), it was felt that the resilient modulus could best characterize pavement material behavior under traffic loads as opposed to other types of material characterizations and therefore that better correlations between performance and computed values could be expected. The various stress-strain relations for different pavement materials included in this study are described in the following paragraphs.

AC

Because of the thermoviscoelastic nature of asphaltic materials, the most important factors influencing the stress-strain relationship of asphaltic materials are temperature and rate of loading. The dynamic modulus E of asphaltic material should be evaluated in the laboratory at different temperatures and at different rates of loading. However, such information for asphaltic mixtures used by the Corps of Engineers was not available during the preparation of this report. Figures 1-3 show complex moduli of three asphaltic mixtures, evaluated at different temperatures and at different rates of loading, determined by Kingham

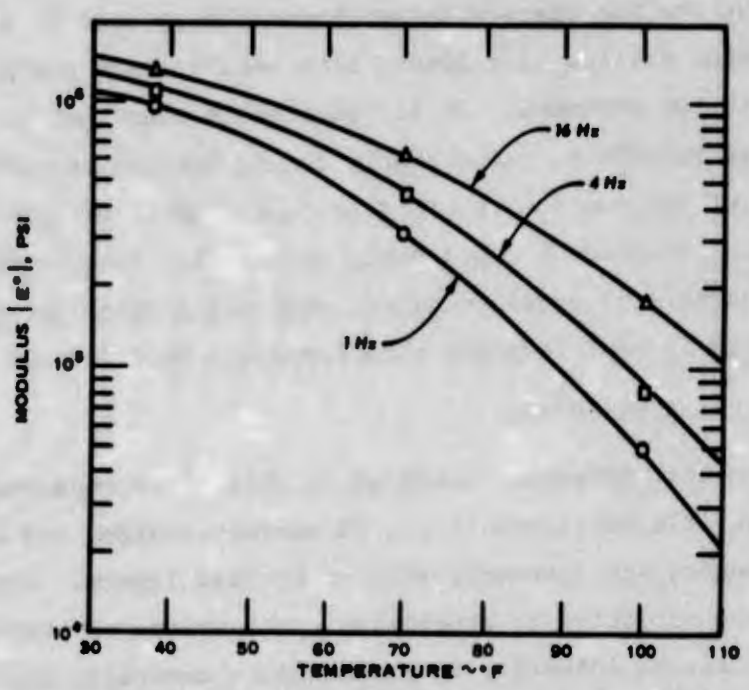

Figure 1. Modulus-temperature relationships for AC base course (courtesy of University of Michigan[4])

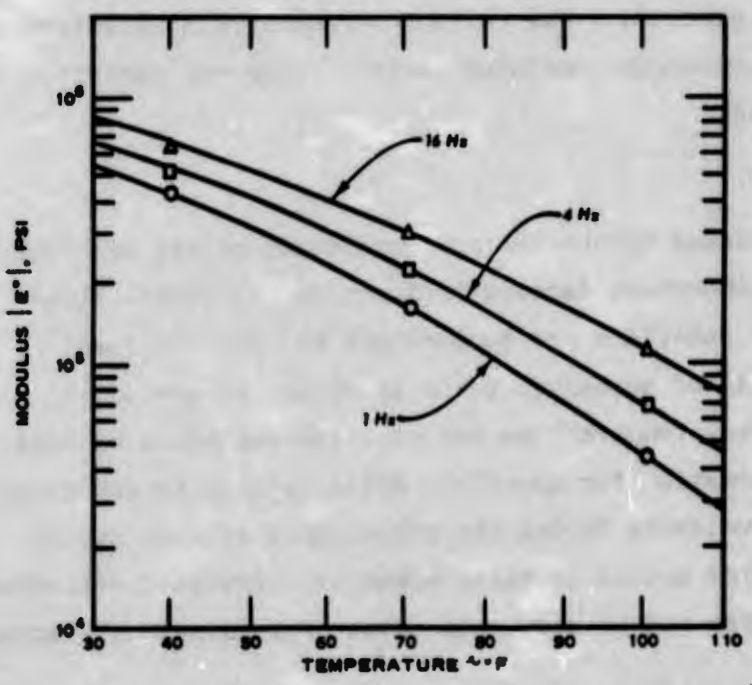

Figure 2. Modulus-temperature relationships for sand-asphalt base course (courtesy of University of Michigan[4])

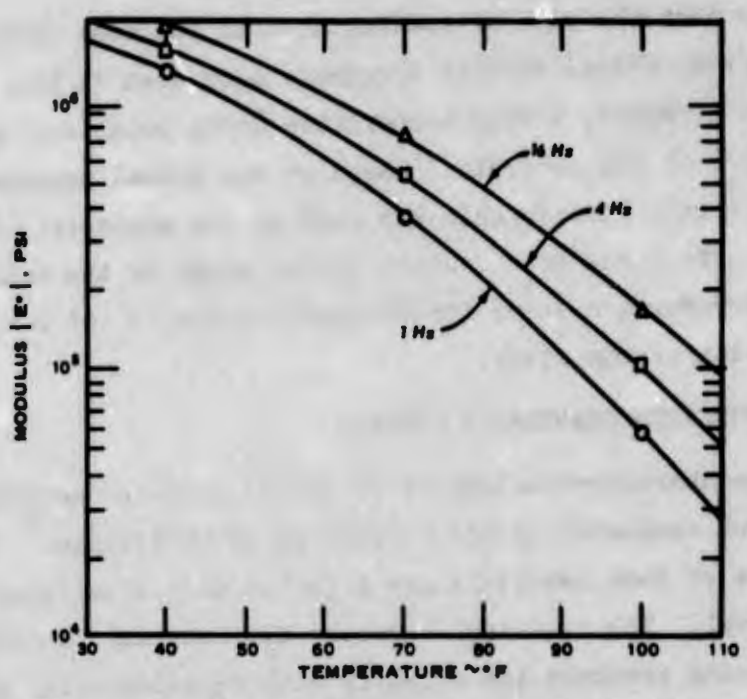

Figure 3. Modulus-temperature relationships for surfacing (courtesy of University of Michigan[4])

and Kallas.[4] Since the patterns of resilient moduli for asphaltic mixtures used by the Corps of Engineers are believed to be similar to those shown in Figures 1-3, the moduli shown in the figures were used in this study. According to Kingham and Kallas,[4] the test condition of 1 Hz

---

* The modulus values for the asphaltic mixtures were obtained from regression equations describing stiffness as a function of temperature and frequency of loading. The speed of the test rig was converted to a frequency of loading by assuming that a point at the bottom of the asphalt layer would be in tension for the length of time it took for a dual wheel to traverse 3 ft. (A table of factors for converting units of measurement is presented on page 4.) (Coffman, Kraft, and Tamayo[5] made a similar assumption but also included the amount of time that the bottom of the asphalt layer was in compression.) Given this assumption, speed in miles per hour is related to frequency in hertz by the formula

$$\text{speed} = \frac{(\text{frequency})(3600)(3)}{5280} = \text{frequency } (2.05)$$

Thus, for a frequency of 1 Hz, this relationship gives a speed of approximately 2 mph.

simulates best the rate of loading used in the test sections; therefore, the resilient moduli at this frequency were used in this study. For each test pavement, a mean temperature-depth relationship during the traffic period was determined based on the actual temperature measurements, and this relationship was used in the analysis. Only limited research effort has been devoted to the study of the volumetric behavior of AC; therefore, a value for Poisson's ratio ν of 0.4 was used in this portion of the study.

UNTREATED GRANULAR MATERIALS

The characterizations of untreated granular materials were based on research conducted at the University of California.[6] The resilient properties of such materials are affected most significantly by the stress level. The resilient modulus M_R increases considerably with the confining pressure and slightly with repeated axial stress. So long as shear failure does not occur, M_R can be approximately related to the sum of the principal stresses θ and to the confining pressure σ_3 (the minor principal stress) by

$$M_R = K_1\theta^{K_2} \qquad \text{(bis 1)}$$

$$M_R = K_3\sigma_3^{K_4} \qquad (3)$$

where K_1, K_2, K_3, and K_4 are material constants. Poisson's ratio ν increases with decreasing σ_3 and increasing repeated axial stress so that the change in ν can be approximated by

$$\nu = A_0 + A_1\left(\frac{\sigma_1}{\sigma_3}\right) + A_2\left(\frac{\sigma_1}{\sigma_3}\right)^2 + A_3\left(\frac{\sigma_1}{\sigma_3}\right)^3 \qquad (4)$$

where

A_0, A_1, A_2, A_3 = material constants

σ_1 = major principal stress

σ_3 = minor principal stress

The constants shown in Equations 3 and 4 reflect the resilient properties of granular material, which are influenced by factors such as aggregate density, aggregate gradation (percent of material passing a No. 200 sieve), aggregate type, and degree of saturation. At a given stress level, M_R increases with increasing density, increasing particle angularity or surface roughness, decreasing fines content, and decreasing degree of saturation. Poisson's ratio, however, is only slightly influenced by density and generally decreases as the fines content and degree of saturation increase.

Some researchers have characterized the granular materials in the form shown in Equation 5.

$$M_R = K_5 + 2K_6\sigma_r \qquad (5)$$

where K_5 and K_6 are material constants and σ_r is the radial stress.

Equations 1 and 3 are capable of characterizing granular materials in a nonlinear fashion, i.e., M_R varies with the state of stress. However, these equations have also been bitterly criticized for the inability to characterize tensile properties of granular materials. In a conventional flexible pavement under heavy loads, it is conceivable that radial tensile stresses would develop at the lower part of the granular base. For most computer programs available at present, an arbitrary small value of M_R close to zero is assigned to the granular material once M_R computed from Equations 1 and 3 becomes negative. In such cases, awkward values of strain components and excessively large displacements result. In this respect, Equation 1 is far superior to Equation 3 for reasons explained in the following paragraph.

In Equation 1, θ is the sum of principal stresses σ_1, σ_2, and σ_3. When radial tensile stresses are computed at the lower portion of the base, the minor principal stress σ_3 becomes negative and causes M_R to become undefined in Equation 3; but, since the major principal stress σ_1 is positive and is much larger than σ_3 under most stress levels, M_R computed by Equation 1 is positive in

most cases. Therefore, the M_R values computed by Equation 1 are more meaningful. In Appendix A, the results computed by Equations 1 and 3 are discussed. Due to the close agreement between measured and computed stresses and deflections (as shown in Appendix A), expressions shown in Equation 1 were used in this study to characterize the resilient properties of granular materials. Table 1 shows values of constants shown in Equations 1, 3, and 5 for various granular materials developed by other researchers.

For the purpose of this study, the representative values shown in Table 1 were first tried. The method for determining the values of these constants will be described in the correlation of theory and performance.

Because of lack of experimental results in volumetric behavior of granular materials, values of ν were not computed by Equation 4. A value of 0.48 was used for both base and subbase materials in this portion of the study. It was believed that, since granular materials in a pavement structure under a thin AC surface tend to expand under heavy aircraft loads, large values of ν would represent field conditions better than small values.

SUBGRADE SOILS

Resilient Modulus. Extensive studies of the behavior of fine-grained materials in laboratory repeated load tests were made by Seed, Chen, and Lee.[8] They found that M_R did not depend on σ_3 but was sensitive to σ_d, the deviator stress. The relationship between M_R and σ_d generally has the shape shown by the curve in Figure 4, which is based on actual tests of a 4-CBR buckshot clay soil at WES. At low stress levels, M_R decreases rapidly with increasing values of σ_d; and as σ_d further increases, there is only a slight increase in M_R. A bilinear material model, developed by Wang, Mitchell, and Monismith,[9] in characterizing a highly plastic subgrade material, has the following expression for M_R in Equations 6 and 7.

Table 1

Material Constant Values Proposed for Various Granular Materials by Other Researchers (After Barker, Brabston, and Townsend[7])

Description	Constants	
Expression: $M_R = K_3\sigma_3^{K_4}$ (Equation 3)		
	K_3	K_4
Dry, partially crushed gravel	10,094	0.580
Dry, crushed gravel	13,126	0.550
Partially saturated, partially crushed gravel	7,650	0.591
Partially saturated, crushed gravel	8,813	0.569
Saturated, partially crushed gravel	9,894	0.528
San Diego base	12,225	0.540
Gonzales Bypass base	15,000	0.480
Gonzales Bypass subbase	10,000	0.400
Morro Bay base	11,800	0.390
Morro Bay subbase	6,310	0.430
Expression: $M_R = K_1\theta^{K_2}$ (Equation 1)		
	K_1	K_2
San Diego base	3,933	0.610
Dry, crushed gravel	2,156	0.710
Partially saturated, crushed gravel	2,033	0.670
Morro Bay subbase	2,900	0.470
Morro Bay base	3,030	0.530
Expression: $M_R = K_5 + 2K_6\sigma_r$ (Equation 5)		
	K_5	K_6
Crushed limestone	4,856	390
Crushed limestone after 36,000 repetitions	37,710	1082

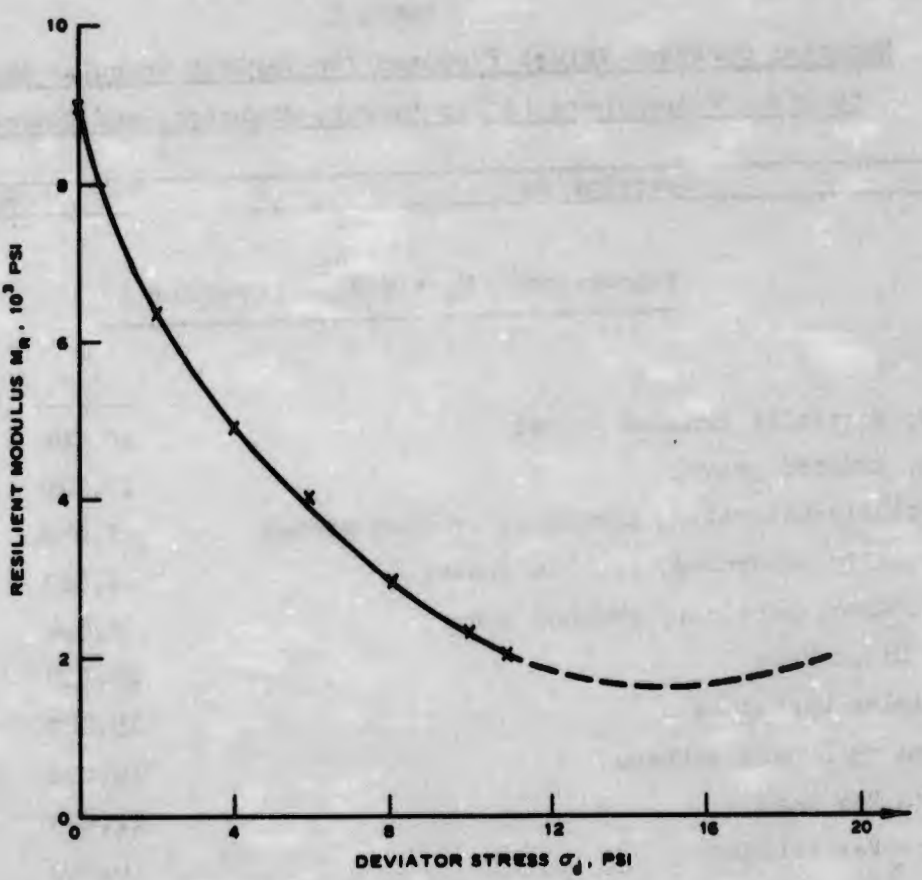

Figure 4. Effect of stress intensity on resilience characteristics of fine-grained soils

$$M_R = K_1 + (K_2 - \sigma_d)K_3 \quad \text{for} \quad \sigma_d < K_2 \tag{6}$$

$$M_R = K_1 + (\sigma_d - K_2)K_4 \quad \text{for} \quad \sigma_d > K_2 \tag{7}$$

The relationship shown in Figure 4 between M_R and σ_d for fine-grained soils has special practical significance. As has been pointed out by Seed, Chen, and Lee,[8] the stress levels to which pavement subgrades are subjected are likely to be in the lower range, in which M_R varies most widely. As the depth of a soil element below the pavement surface increases, σ_d will progressively decrease; thus, even if the soil is completely uniform, M_R will in fact increase with depth. This

variation will clearly complicate the application of linear elastic theories developed for conditions of uniform moduli for the computation of resilient pavement deflections and will also require careful consideration in the selection of a single modulus value for incorporation in such theories. It also indicates that the contribution of the upper layers of a compacted clay subgrade to the total resilient subgrade deflection will be far greater than is indicated by linear elastic theory.

Static Modulus. Another mathematical model characterizing the stress-strain relationship for soils is that developed by Duncan and Chang.[10] The model is derived based on the assumption of a hyperbolic stress-strain relationship and the Mohr-Coulomb failure criteria. The tangent modulus E_t under any stress condition is expressed as

$$E_t = \left[1 - \frac{R_f(1 - \sin \phi)(\sigma_1 - \sigma_3)}{2C \cos \phi + 2\sigma_3 \sin \phi}\right]^2 E_i \qquad (8)$$

where

$R_f = \dfrac{(\sigma_1 - \sigma_3)_f}{(\sigma_1 - \sigma_3)_{ult}}$ where $(\sigma_1 - \sigma_3)_f$ is the principal stress difference at failure and $(\sigma_1 - \sigma_3)_{ult}$ is the ultimate stress difference at failure

$(\sigma_1 - \sigma_3)$ = deviator stress

C and ϕ = Mohr-Coulomb strength parameters

E_i = the initial tangent modulus from the $(\sigma_1 - \sigma_3) \sim \varepsilon$ curve

Equation 8 represents the nonlinear, stress-dependent, inelastic stress-strain behavior of soils and is convenient for use with the finite element method of analysis. The parameters C , ϕ , R_f , and E_i can be readily determined from results of standard laboratory triaxial tests. Equation 8 was used to characterize the subgrade soil of a test pavement. The computed results are presented in Appendix A.

Relations Between Dynamic Modulus of Elasticity and CBR. In earlier work by Heukelom and Foster,[11] a simple relationship was found

between the dynamic modulus of elasticity E and CBR which is expressed as

$$E = 1500\ CBR \tag{9}$$

As explained earlier in this section, when pavement materials are subjected to repetitive applications of traffic loads and the stress intensities in the subgrade are small (well below failure strengths of the subgrade soil), M_R as determined by Equations 6 and 7 should best characterize soil behavior in the real pavement system. However, M_R values for subgrade soil were available only for 4-CBR buckshot clay. Therefore, Equation 9 was used to determine the M_R of subgrade soils in the study. A value for ν of 0.4 was used in the computations. Attempts were not made to back-calculate the nonlinear constants in Equations 6 and 7 because of the complexities of the work involved.

DEFICIENCIES OF MATERIAL CHARACTERIZATION

The success of the finite element method lies primarily in the correctness of stress-strain relations of materials inputed to the program. Much research effort has been spent in this direction, but continuing endeavors are still needed. The deficiencies of stress-strain relations of pavement materials developed based on present-day knowledge and available testing equipment are discussed in the following paragraphs.

Inadequacy of Laboratory Testing Conditions. The constitutive relationships determined in the laboratory do not truly characterize pavement material properties under actual field conditions. The laboratory triaxial tests apply repeated axial and radial stresses, and the resulting strains are measured. Although these tests fairly well define the constitutive relations for pavement materials at points beneath the load axis of a single wheel (assuming the case of axisymmetry is valid), the results are inadequate for conditions elsewhere in the pavement. The inadequacy occurs because the triaxial test permits only two normal

stresses to be varied and the resulting two strains to be measured, while the complete characterization of the materials outside the axis of symmetry requires three normal stresses and one shear stress and the resulting four strains. The condition becomes more complicated for multiple-wheel loads since it becomes necessary to measure all six strains induced by all possible combinations of three normal and three shear stresses.

Significance of Poisson's Ratio. The precise determination of Poisson's ratio of pavement materials is of vital importance in formulating appropriate constitutive relations. For a linearly elastic material, it is true that the computed vertical stresses depend very little on ν ; however, this does not necessarily mean that the response of the pavement to loads is insensitive to the volume change of the material. In fact, when the constitutive relation of a material is mathematically formulated by a second-order (nonlinear) polynomial,[12] the modulus of the material depends very much on the manner in which the material changes its volume. Unfortunately, due to lack of knowledge of volume change behavior of pavement materials, constant values of ν determined in an arbitrary manner are generally used in the nonlinear finite element analysis. Such was the case in this study. Although Equation 4 gives the value of ν quantitatively the equation is still subject to the limitations of the testing conditions.

Assumption of Isotropy of Pavement Materials. Isotropy assumes that a material has identical properties in all directions. This assumption is undoubtedly not true in view of field compaction procedures. However, the concept of anisotropy of materials has not been practicable in analytical analysis of pavement structures because of practical difficulties, i.e., difficulties in mathematical formulation of equations, numerical analysis of equations, and determination of material constants in the laboratory. In the finite element program used in this study, material isotropy was assumed.

Tensile Properties of Pavement Materials. Equations 1, 3, and 5-7 express the magnitude of the M_R of materials determined under laboratory compression states of stress. To date, the tensile properties

of pavement materials are not very well known to pavement engineers. While indirect tensile tests and simple supported beam tests can qualitatively describe the tensile properties of materials, the tests hardly represent actual field conditions. The inability of Equations 1 and 3 to determine the M_R of granular materials when radial tensile stresses are developed in the lower part of the granular base was discussed previously. It is certain that knowledge of tensile properties of materials can greatly improve the accuracy of the finite element technique.

CORRELATION OF THEORY AND PERFORMANCE

In this part, the concept and computational procedure described in the previous part will be applied to the analysis of performance data from full-scale accelerated traffic tests. Tables 2 and 3 show test data from several selected test sections for single- and multiple-wheel loads, respectively; the data cover a broad spectrum of loads, gear configurations, pavements, subgrade soils, and coverage levels. The failure criteria* from which the coverage levels were determined were based primarily on the surface condition of the pavements. One coverage is defined to be the number of passes of load tires in adjacent tire paths sufficient to cover a given width of surface area a single time. The moving test loads were nearly normally distributed along the cross section of the traffic lane.

In the finite element program used in this study, the stress components were computed at the center of each element, and the displacement components were computed at grid points. The horizontal strains along interfaces were computed as the difference in horizontal displacement at two adjacent grid points divided by the distance between the points. The vertical strains in each element were determined similarly. Stress components and vertical strains along interfaces were determined from the other computed points by extrapolations. The continuity conditions along interfaces which should be observed during extrapolation are shown in Equation 2.

The computer program used in this study assumes that the pavement structure is an elastic medium with nonlinear stress-strain characteristics. The computed stress, strain, and displacement are therefore the response of the pavement to the load before initial failure occurs, or

---

* The present failure criteria are defined as either of the following conditions:

a. Surface upheaval of 1 in. or greater of the pavement adjacent to the traffic lane.

b. Severe surface cracking to significant depths such that the surface is no longer waterproof.

Table 2

Single-Wheel Test Data

Reference	Test Pavement	Wheel Load kips	Tire Contact Area, sq in.	Thickness, in.			Subgrade CBR*	Observed Coverages at Failure
				Surface	Base	Subbase		
13	1	200	1500	7.0	13.0	19.0	6.0	150
13	2	200	1500	7.0	15.0	21.5	9.0	1700
13	3	200	1500	6.0	13.0	30.0	8.0	1300
13	4	200	1500	6.0	12.0	0.0	16/6 (41.5 in.)	10
13	5	200	1500	6.5	14.0	0.0	18/6 (45.5 in.)	60
13	6	200	1500	6.5	14.5	25.0	15.5/6 (39.5 in.)	360
13	7	200	1500	7.0	14.0	9.0	17.5/6 (34.0 in.)	1500
14	8	30	150	3.0	6.0	6.0	14.0	216
15	9	15	250	2.0	8.0	0.0	8.0	3760
15	10	15	250	2.0	8.0	0.0	9.0	3760
16	11	50	285	3.0	6.0	6.0	3.7	6
16	12	30	285	3.0	6.0	6.0	3.7	120
14	13	30	150	1.5	10.5	0.0	7.0	178
14	14	30	150	2.0	10.0	0.0	6.0	203
17	15	10	91	0.0	5.0	0.0	6.0	40
15	16	50	667	3.0	23.0	0.0	5.0	3000
15	17	20	334	3.0	14.5	0.0	5.0	5000
15	18	15	250	2.0	0.0	10.0	5.0	582
15	19	25	416	2.0	4.0	12.0	5.0	385
18	20	75	270	15.0	0.0	0.0	4.0	6
18	21	75	270	15.0	0.0	0.0	4.0	8
16	22	50	285	3.0	6.0	15.0	4.0	200
18	23	75	270	9.0	0.0	15.0	4.0	12
18	24	75	270	24.0	0.0	0.0	4.0	90
19	25	75	270	3.0	21.0	0.0	4.0	50

* Single entries indicate a CBR that is representative of the entire depth of test; double entries indicate a change of CBR with depth (e.g., for test point 4, the upper 41.5 in. of subgrade had a CBR of 16; below that depth a CBR of 6 was representative).

Table 3

Multiple-Wheel Test Data

Reference	Test Pavement	Aircraft* Type	Assembly Load kips	Tire Contact Area, sq in.	Thickness, in. Surface	Base	Subbase	Subgrade CBR	Observed Coverages at Failure
16	1	Boeing 747	240	290	3	6	24	3.8	40
16	2	Boeing 747	240	290	3	6	24	4.0	40
16	3	Boeing 747	240	290	3	6	32	4.0	280
16	4	C-5A	360	285	3	6	6	3.7	8
16	5	C-5A	360	285	3	6	24	3.8	1500
16	6	C-5A	360	285	3	6	24	4.0	1500
18	7	C-5A	360	285	3	12-in. asphalt stabilized		4.0	98
18	8	C-5A	360	285	15	0	0	4.0	425
16	9	C-5A	360	285	3	6	15	4.0	104
18	10	C-5A	360	285	9	0	15	4.0	734
18	11	C-5A	360	285	9	15-in. asphalt stabilized		4.0	2198
19	12	C-5A	360	285	3	21	0	4.0	5000
19	13	Boeing 747	200	285	3	21	0	4.0	890

* Tests were performed using a twin-tandem assembly, which represented one twin-tandem component of the Boeing 747 assembly, and a 12-wheel assembly, which represented one main gear of a C-5A assembly.

preferably during the early stages of traffic. The performance of the full-scale test sections under traffic, however, is based on the integral pavement behavior up to the point of functional failure. Therefore, the use of finite element programs to predict pavement behavior during the early stages of traffic is reasonable but is not totally acceptable for predicting failure coverages of pavements. In fact, there is not a single computer program available at present which is capable of predicting failure of a pavement in a simple and straightforward manner. Therefore, efforts were combined in this study to correlate the computed values and the actual observed coverages to failure of the test pavement. Such correlations could be identified from the parameters controlling the pavement performance. This approach was based on the hypothesis that correlations must exist between performance of the pavement and the actual developed stresses and strains in the pavement under the load. Since the stresses and strains have to be computed theoretically, the success of the correlation depends entirely upon the accuracy of the stress-strain relations of pavement materials inputed into the computer program. It is apparent that the closer the representation of material properties, the better the correlations will be.

The stress-strain relations of pavement materials used in this study were presented in the previous part. In the following paragraphs, the rationale for determining the granular material constants K_1 and K_2 in Equation 1 are presented.

The test pavements analyzed (see Tables 2 and 3) were generally of the following three basic types:

a. ABC pavement resting on 4-CBR buckshot clay subgrade soil.

b. Conventional flexible pavements consisting of a 3-in. AC layer, a 6-in. base course, a subbase layer of variable thickness, and subgrade soils of variable CBR's. In most cases, the thickness of the subbase layer is much greater than that of the base, and therefore the subbase layer controls the performance of the pavement.

c. Thick crushed-stone base course pavements with a 3-in. AC layer and subgrade soils of variable CBR's.

If improper stress-strain relations of pavement materials were used in the computation of these three different types of pavements, it

is probable that good correlations between computed values and performance could not be obtained. More than likely, three different correlations would result. On the other hand, if correct stress-strain relations were used, a single good correlation should be obtained for the three types of pavements. Based on this principle, the values of K_1 and K_2 in Equation 1 were determined.

Since all the ABC pavements (multiple wheels) were constructed over 4-CBR subgrade soil, good correlations between computed values and performance were first established. Computations on conventional flexible pavements and full-depth base course pavements were subsequently made. K_1 and K_2 in Equation 1 were assumed to be 2900 and 0.47, respectively, for subbase materials and 3933 and 0.61, respectively, for base course materials. It was found that correlations for conventional flexible pavements compared very well with those for ABC pavements, but the correlations for thick base course pavements did not. The computed stresses and strains for thick base course pavements were much too large. This indicates that the constants K_1 and K_2 chosen for subbase materials were reasonable but were too small for base course materials. High values of K_1 and K_2 were tried in an effort to obtain good correlations, and the resulting values were 8300 and 0.71, respectively.

SINGLE-WHEEL TEST DATA

Table 2 shows test data for 25 selected test pavements. The base course materials were generally well-compacted crushed stone, and the subbase materials were generally gravelly sand.

Pavements 20, 21, and 24 were ABC, but contained different base courses. Pavement 20 was composed of a 3-in. layer of AC surface course (4.5 percent asphalt) and a 12-in. layer of bituminous-stabilized gravelly sand with a 6.5 percent cement filler base course. Pavement 21 had the same layer of AC surface course plus a 6-in. layer of surface-mix (5.0 percent asphalt) base course and a 6-in. layer of surface-mix (2.9 percent asphalt) base course. The top 9 in. of pavement 24 was the same as that of pavement 21, but the bottom 15 in. was a layer of bituminous-stabilized gravelly sand (2.9 percent asphalt).

For each test pavement, a mean temperature-depth relationship during the traffic period was estimated, and the corresponding resilient moduli were obtained from Figures 1 and 2 for computations. Test pavement 22 was tested at two different ambient temperature conditions: one was between 60 and 70°F and the other between 90 and 115°F. The observed performances for the two conditions were identical, indicating that the 3-in. temperature-dependent AC surface layer had little effect on the performance of the pavement. The results presented are based on an analysis of cooler period conditions.

Figure 5 shows the relationships between vertical strain ε_v at the subgrade surface and performance. Figure 6 shows relationships between radial tensile strain ε_r at the bottom of the AC layers and performance. Uncertainties exist in the computed values of pavements with high CBR subgrade soils; these were pavements 4-8 represented in the figures by open circles. In the discussion to follow, these pavements are excluded; they will be treated later in this report.

In Figure 5, the best-fit line was drawn through data points for all pavements with coverage levels greater than 100. It would seem that

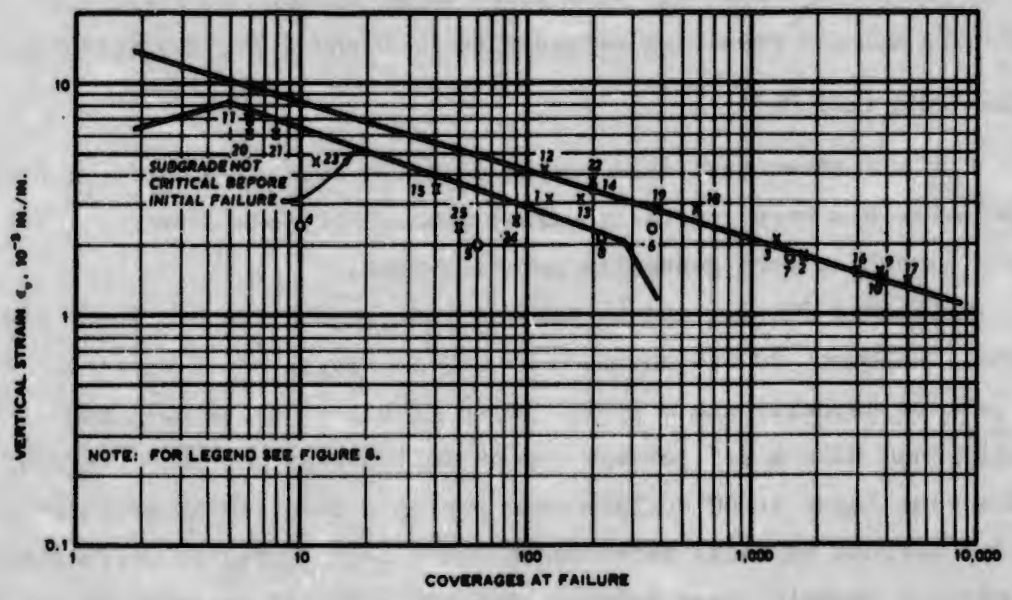

Figure 5. Relationships between vertical strain at the subgrade surface and performance of the pavement system under single-wheel loads

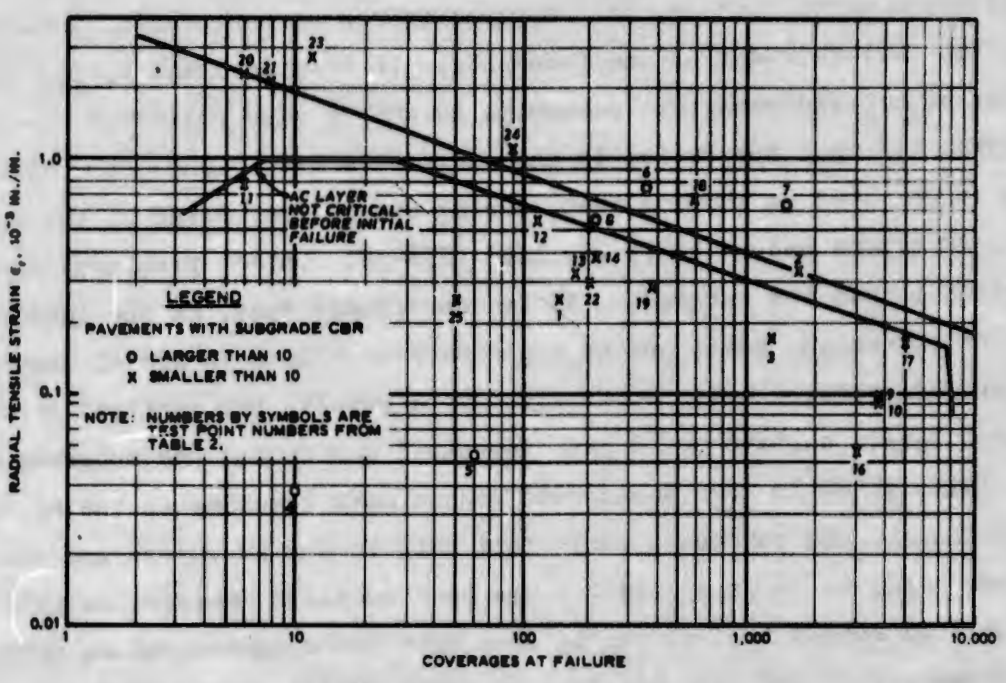

Figure 6. Relationships between radial tensile strain at the bottom of the AC and performance of the pavement system under single-wheel loads

another line could be drawn through the data points for pavements with coverage levels less than 100. In view of the distribution of pavement data points in Figure 6, it was concluded that, for pavements with coverage levels less than 100, the subgrade condition was not critical before initial failure occurred; rather, it was the radial tensile strain at the bottom of the AC layer that was critical. The line of best fit in Figure 6 was drawn accordingly and passes through the point for test pavement 2, which sustained 1700 coverages before failure. Failure test data, however, were insufficient at high coverage levels; therefore, the validity of the criteria established for these levels needs further verification by more field performance studies. The radial tensile strains for pavement points below the line were not considered to be critical before initial failure.

As discussed earlier in this section, the computer program used to compute the stresses and strains of the pavement assumes that the pavement is an elastic medium. The computed values give an indication of the response of the pavement structure to the load before initial

failure occurs; however, the computed values do not provide information on the failure modes of the pavements. In Figures 5 and 6, for example, they do not indicate that pavements 20 and 21 were failed in the AC layers but were not failed in the subgrade soils; rather, the data should be interpreted as showing that, during the initial stage of the traffic, the AC layers under the 75-kip load (278-psi contact pressure) were more critical than the subgrade. It is conceivable that, as the load repetitions increased, small cracks could have developed in the AC layers and therefore reduced their stiffness. As a result, the vertical strain at the subgrade surface would have increased and caused the subgrade soil to fail, which in turn would have caused more cracking in the AC layer. Eventually, the pavements would fail both in the AC layers and the subgrade soil, as was the case for the test sections analyzed in this study. From this discussion, it can be seen that the computed values provide information on the critical factors contributing most to the pavement failures, rather than indicating the failure modes of the pavement under the load.

The results of analysis for unbound granular materials are presented in Figures 7 and 8. The ABC pavements 20, 21, and 24 are not shown in this plot. Figure 7 shows the plotted results for maximum radial tensile strains. The locations of the maximum strains were generally near the load axis but varied in depth (as indicated by the computer output). The line of best fit was drawn based on the following reasoning: Since the failure coverages of pavements 1, 2, 12, 18, and 19 could be predicted by the correlation of subgrade vertical strains in Figure 5, it is reasonable to assume that the failure coverages of these pavements should be at least equal to or greater than those predicted by the criteria for shear failure in the unbound granular materials. The line of best fit was therefore drawn through these pavement points. It is interesting to note that the line also passes through pavement points 15 and 11. Pavement 15 had no AC surface course but did have a 5-in. crushed-stone base placed on 6-CBR subgrade soil. Figure 5 indicates that the failure of this pavement did not initiate in the subgrade soil. Since this pavement had no other component layer but the granular

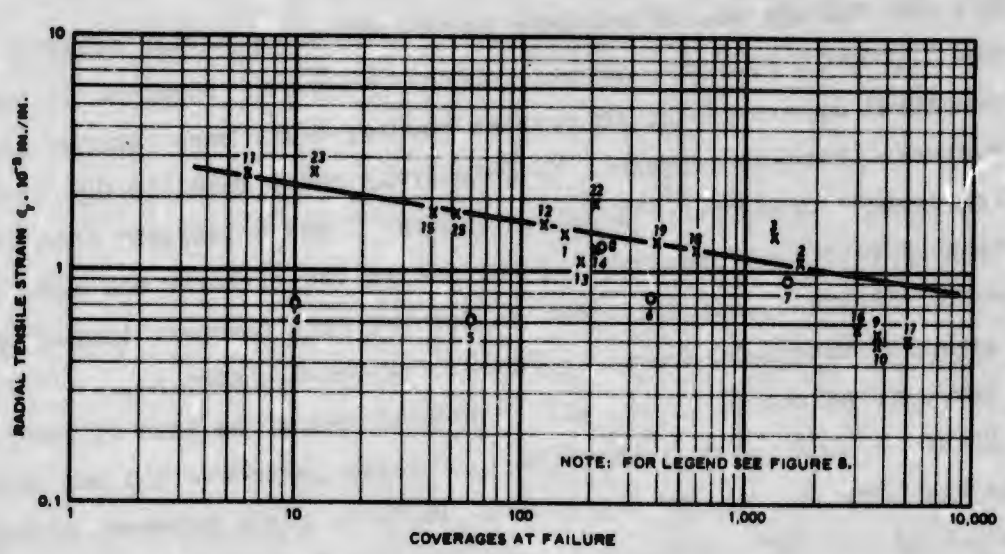

Figure 7. Relationship between maximum radial tensile strain in the unbound granular materials and performance of the pavement system under single-wheel loads

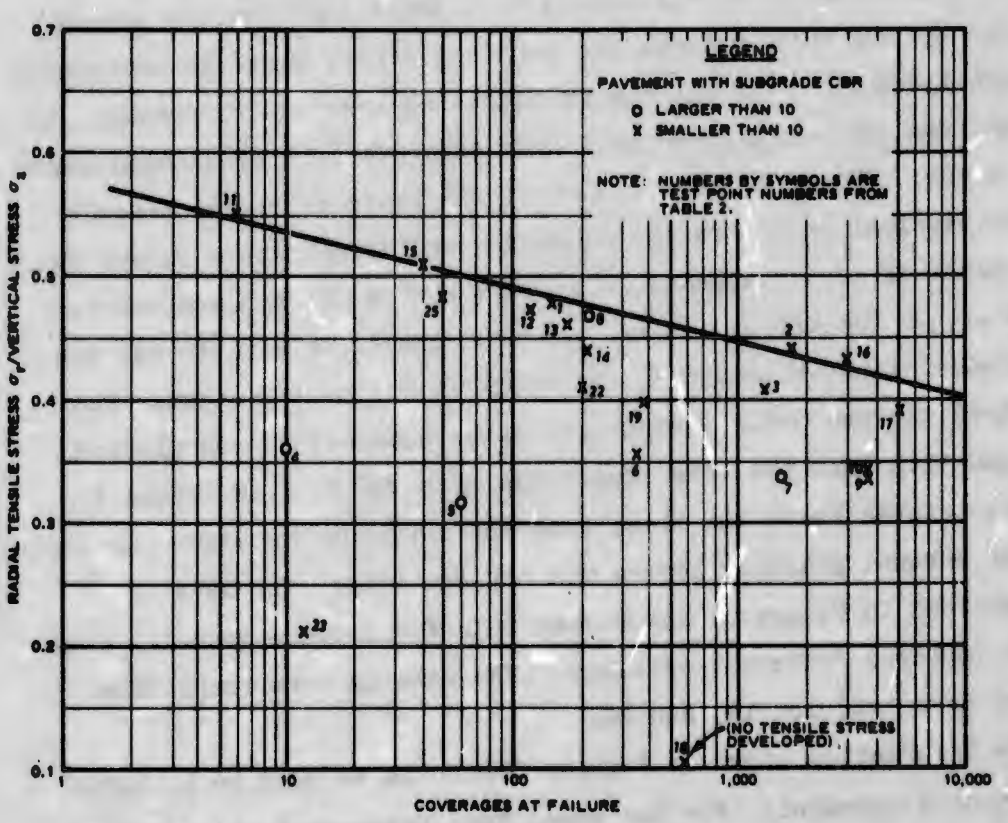

Figure 8. Relationship between the ratio of radial tensile stress to vertical stress in the unbound granular materials and performance of the pavement system under single-wheel loads

material, the failure had to initiate in the unbound granular material under the 10,000-lb load and 110-psi contact pressure. Pavement 11 had thin structural layers (3-in. AC surface course, 6-in. base course, and 6-in. subbase), but was subjected to relatively heavy load (50,000 lb) at a high contact pressure (175 psi). Figures 5 and 6 indicate that the initiation of failure of pavement 11 was not in the AC layer and subgrade soil. Figure 7 indicates that failure of this pavement initiated in the granular materials due to the excessive tensile strains.

Pavement points 7, 9, 10, and 13 plotted below the line of best fit in Figure 7, indicating that failure of these pavements did not initiate in the unbound granular materials. In fact, these pavement points all plot along the curve of the vertical strain criterion in Figure 5.

Because of the possibility of shear failure of unbound bases induced by tensile stresses, Brown and Pell[20] suggested that the design criteria for unbound materials should be a horizontal tensile stress which does not exceed 0.5 times the vertical stress plus the horizontal overburden pressure. For all the pavements analyzed in this study, it was found from the computer outputs that shear failure of unbound bases did not occur. Figure 8 shows a plot of the ratio of radial tensile stress to vertical stress in the unbound granular materials versus failure coverages of test pavements. The ratios were the maximum values selected within the unbound bases. In most cases, this ratio and the maximum radial tensile strain do not occur at the same element. The line of best fit was drawn through the upper boundary of the plotted points, and this line was very compatible with the line in Figure 7. The points located below the lines were the pavements in which the shear failure of unbound granular layers was not critical. The sets of results plotted in Figures 7 and 8 were both for unbound granular materials but employed different criteria. The results were compatible except for pavements 16, 19, and 22.

The information shown in Figures 5-8 could be used to optimize the design of a pavement. For instance, test pavement 2 had an optimum design because the subgrade, the AC surface layer, and the unbound base were all critical at the first application of the 200-kip wheel load.

The computed results were questionable in test pavements 4-8, which had high CBR subgrade soils ranging from 14 to 18. They are represented in the figures by open circles and were not considered in drawing the lines of best fit. The computed values for pavements 4 (CBR = 16) and 5 (CBR = 18) were much too low in Figures 5-8, indicating that the moduli computed by the relation $E = 1500\ CBR$ were too high. However, the computed results for pavements 6 (CBR = 15.5), 7 (CBR = 17.5), and 8 (CBR = 14) seem to fit the line fairly well, indicating that the relation $E = 1500\ CBR$ was adequate. This situation is somewhat puzzling. Nevertheless, two comments on the relation $E = 1500\ CBR$ at high CBR values may be justified: (a) the modulus determined from the relation $E = 1500\ CBR$ seems to be too high for high CBR subgrade soils, and (b) the CBR test may not be a valid test for soils which contain granular particles. For the test condition in which large particles are located beneath the cylinder, the CBR determined can be excessively high and misrepresent the true condition of the soil.

Figure 9 shows the relationship between surface deflection and performance. The plotted results are scattered*, indicating that surface deflection alone is not a good indicator of pavement performance. It is suggested that the shapes of deflection basins should be accounted for in establishing a design criterion. This is manifested by the plotted deflection basins shown in Figure 10. The performance of pavements 2, 12, and 15 as predicted by the surface deflection criterion in Figure 9 would, respectively, be less than, equal to, and more than that actually observed. The deflection basins shown in Figure 10 for these pavements are distinctly different and fully explain the reason for the scattering shown in Figure 9. Evidently, a flatter deflection basin for a pavement means that there is less shearing strain under the load and therefore better performance. Pavement 15 was composed of a 5-in.

---

* Results plotted in Figures 5-8 are also scattered, but straight lines can be drawn through data points in the upper bound for design purposes. The lines can indicate which critical parameter initiated pavement failure. However, such a line can not be drawn between surface deflection and performance as shown in Figure 9.

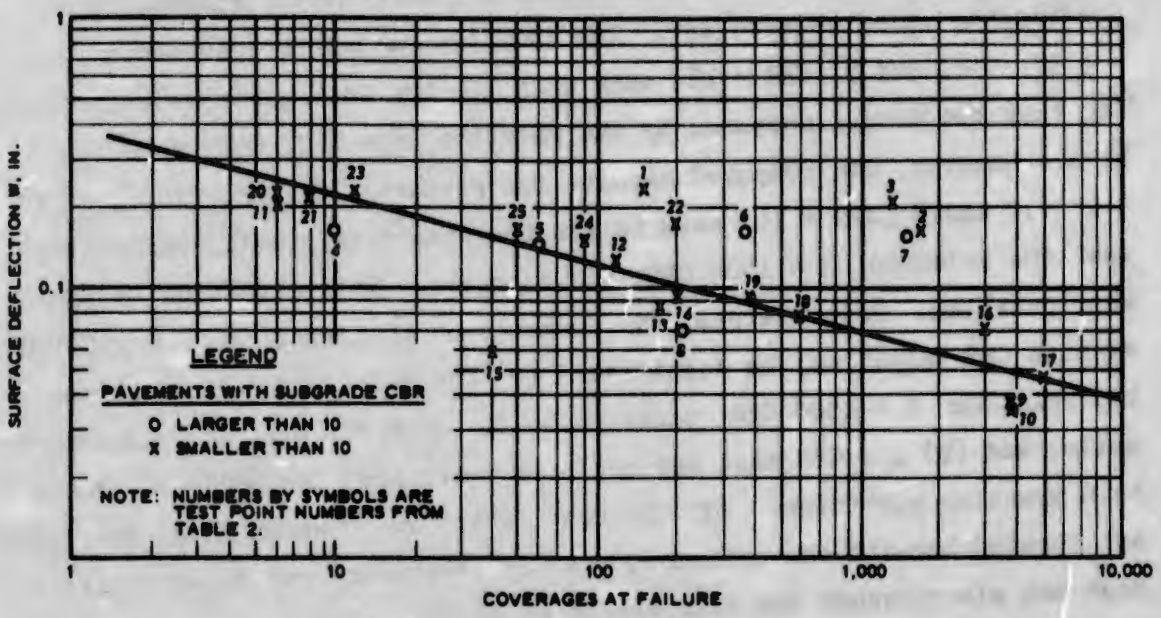

Figure 9. Relationship between surface deflection and performance of the pavement system under single-wheel loads

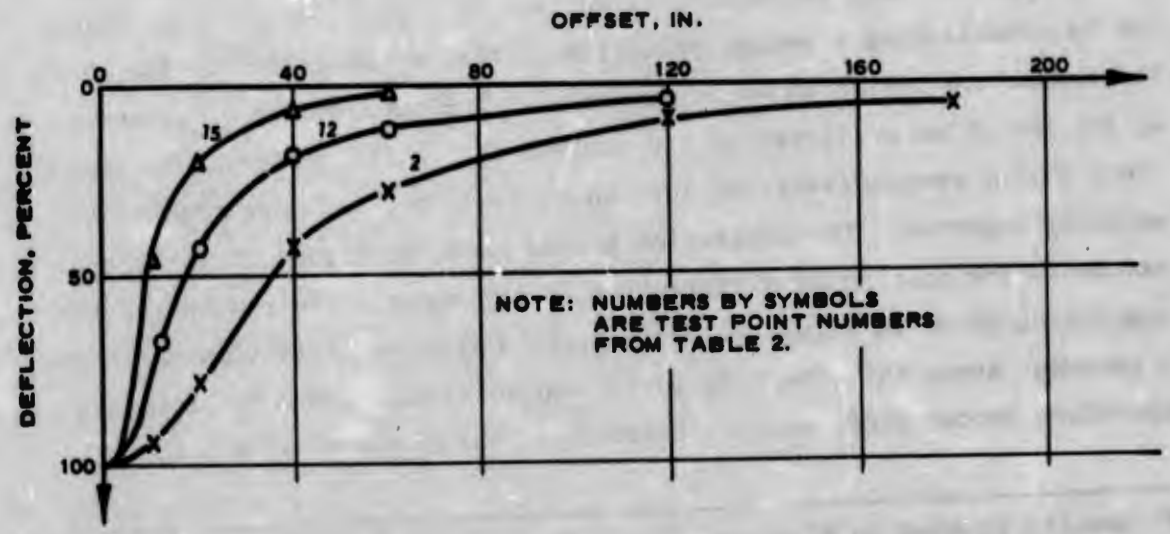

Figure 10. Comparisons of the shapes of deflection basins

unbound crushed-stone base on a 6-CBR subgrade soil without the protection of an AC surface layer. It is conceivable that the surface deflection of this pavement was very steep under the wheel load.

MULTIPLE-WHEEL TEST DATA

Table 3 shows test data for 13 selected pavements tested under multiple-wheel heavy gear loads. The nonlinear finite element computer program used in this study is not capable of handling multiple-wheel loads. Therefore, the superposition principle was used in this study to obtain solutions for multiple-wheel loads. This was done by first constructing the stress basin under a single-wheel load and then superposing the ordinates for different wheels. A computer program was prepared to compute the stresses and strains at any location under the multiple-wheel loads. Discussion of the validity of the superposition principle is presented in References 3 and 21. The principle of superposition has certain limitations, which are explained in the following paragraph.

Application of the superposition principle is justified when the materials being analyzed possess linear characteristics, e.g., AC and/or stabilized materials under certain conditions. For unbound granular materials, however, the stiffness of the material increases with an increase in the stress intensity (confining pressure). Under multiple-wheel loads, it is conceivable that the modulus of unbound granular materials could be higher than that under single-wheel loads. Consequently, the computed value should generally be smaller than that used with the superposition principle. Also, the thicknesses of the unbound bases of the test pavements varied, and this factor could have contributed to the scattering of results shown in Figures 11 and 12.

There is another problem in computing stresses and strains under multiple-wheel loads. Under multiple-wheel loads, the maximum stress and strain occur under the wheel at shallow depths; as the depth increases, the location of the maximum stress and strain moves toward the centroid of the gear assembly. A search for maximum values is tedious and laborious. In this study, the values computed along the load axis of one wheel were used, instead of searching for the maximum. For the

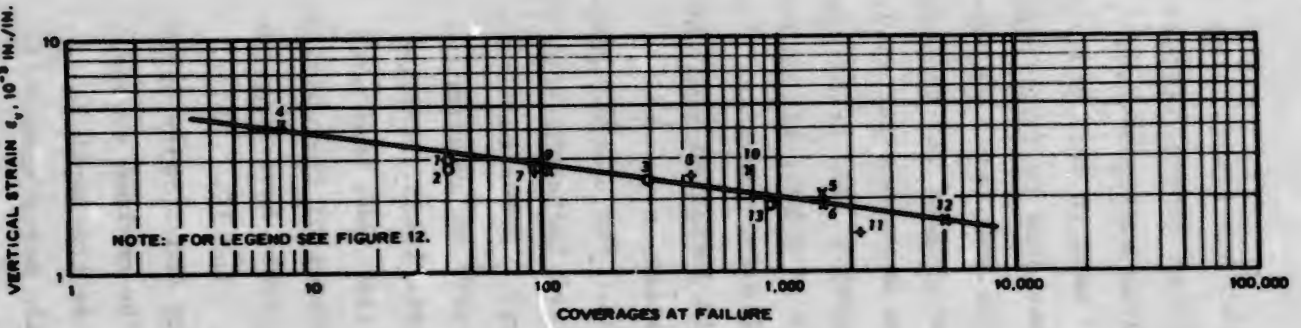

Figure 11. Relationship between vertical strain at the subgrade surface and performance of the pavement system under multiple-wheel loads

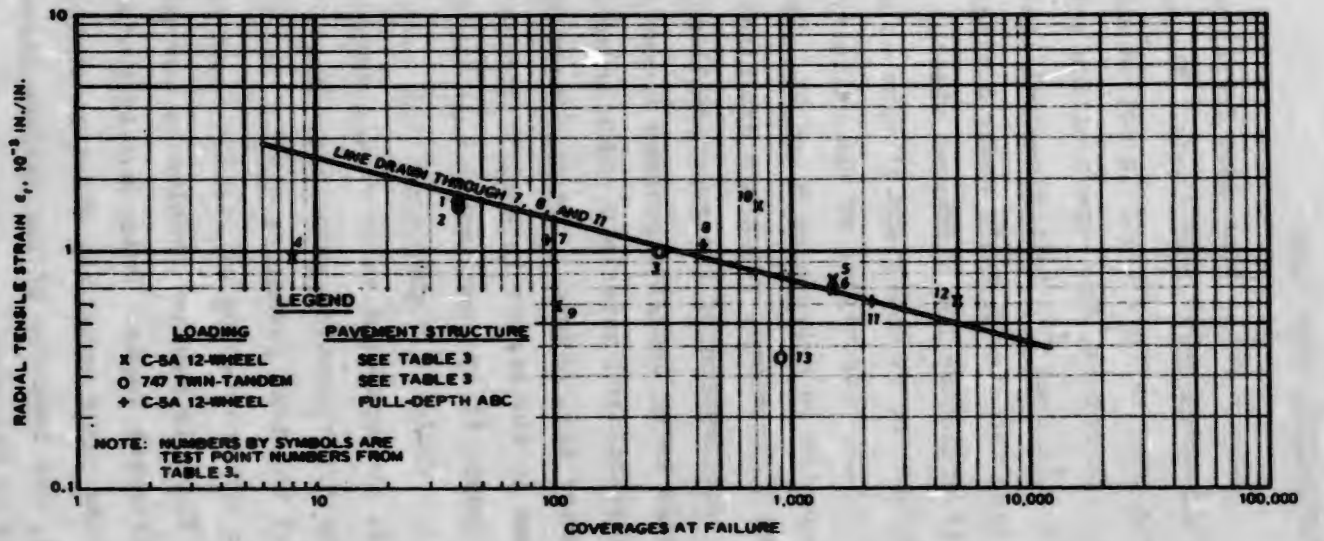

Figure 12. Relationship between radial tensile strain at the bottom of the ABC and performance of the pavement system under multiple-wheel loads

C-5A gear assembly, the wheel was chosen to be either one of the inner wheels in the second row of the 12-wheel assembly. When computations are made at greater depths, it should be noted that the values so computed are smaller than the real maxima. This could be one of the factors contributing to the scattering of results shown in Figures 11 and 12.

Figure 11 shows the relationship between vertical strains at the subgrade surface and failure coverages. Data for the pavements with stabilized layers are not shown in this plot. A straight line could be drawn through pavement points at all coverage levels; thus, the correlations indicate that the performance of this pavement component under multiple-wheel loads could be predicted by the computed values of vertical strain at the subgrade surface. It should be noted, however, that the correlation shown in Figure 11 is not to be interpreted as indicating that all of these pavements were failed in the subgrade soil.

Figure 12 shows the relationship between radial tensile strain at the bottom of the AC layers and performance of the test pavements. Computations showed that the radial tensile strain at the bottom of a thin 3-in. AC surface layer under a single-wheel load was almost the same as the strain under one wheel of the multiple-wheel load assembly due to the AC layer being so thin and the wheels being spaced so far apart. For the ABC pavements, on the other hand, each of the multiple wheels contributed to the radial tensile strain at the bottom of the thick AC layer; this strain was higher than the strain under one wheel. Therefore, it is believed that radial tensile strain in the thin AC layer pavement should not be considered as the controlling factor in the prediction of pavement performance. Therefore, the bottom line in Figure 12 was drawn through the points for ABC pavements 7, 8, and 11, without considering pavements 1-6, 9, and 13, which were the conventional flexible pavements with 3-in. AC surface courses. It can be seen that computed radial tensile strains in pavements 1, 2, 4, 9, and 13 were smaller than those of the ABC pavements because of the nature of the thin AC layers. For pavements 1-3, 5, 6, and 14, however, the points fell rather close to the line; but the closeness was considered to be only coincidental. The reason for pavement point 10 being located

so far up the line is not known. One possible explanation is that the temperature of the 9-in. AC layer input into the computer program for computation could have been incorrect.

The results presented in Figures 11 and 12 are limited to 4-CBR subgrade soils. The question arises as to whether the criteria established are applicable to other subgrade soils. In view of the criteria established for single-wheel loads presented in Figures 5-8 in which the results for low-CBR subgrade pavements were consistent with those for higher CBR subgrade pavements, it is justified to conclude that the correlations presented in Figures 11 and 12 for multiple-wheel loads can be used for pavements other than those on 4-CBR subgrade soils.

A criterion for shear failure in unbound granular materials was not established for pavements subjected to multiple-wheel loads. This was due to the practical difficulty in searching for the maximum radial tensile strain (Figure 7) and the maximum stress ratio (Figure 8) in the unbound layers when the principle of superposition was used.

CONCLUSIONS AND RECOMMENDATIONS

CONCLUSIONS

Resilient moduli of unbound granular materials have been back-calculated from the good correlations established from the computed parameters and observed performance of many accelerated traffic test pavements. The parameters are the vertical strain at the subgrade surface, shear force in the unbound granular layers, and radial tensile strain in the AC layer. With reference to Equation 1, the K_1 and K_2 values so determined were 8300 and 0.71, respectively, for base materials and 2900 and 0.47, respectively, for subbase materials. The moduli so determined represent the average values of granular materials used by the Corps of Engineers.

It was found that the surface deflection alone is not a good indication of pavement performance and thus should be combined with other parameters, such as the shape of the deflection basin.

Good correlations were obtained for pavements with low- and medium-CBR subgrade soils when the relation $E = 1500\ CBR$ was used in the analysis; however, they were not obtained for pavements with high-CBR subgrade soils.

The measured stresses and deflections obtained in one of the multiple-wheel heavy gear load test sections for single-wheel loads agree well with computed values from the finite element program. The nonlinear moduli of granular materials were evaluated from accelerated traffic test data (Appendix A).

RECOMMENDATIONS

The nonlinear resilient moduli of granular materials presented in this report can be used in the iterative layered elastic computer program to compute pavement responses when laboratory repeated load test data on granular materials are not available. The iterative layered elastic computer program may be found in Reference 21.

APPENDIX A: COMPARISONS OF COMPUTED AND MEASURED STRESSES AND DISPLACEMENTS

In this portion of the study, the vertical stresses and displacements measured in item 3 of the multiple-wheel heavy gear load test section[22] at the U. S. Army Engineer Waterways Experiment Station (WES) were compared with those computed by the nonlinear finite element method incorporated with various nonlinear stress-strain relations of the pavement materials. The multiple-wheel heavy gear load test section was composed of a 3-in. asphaltic concrete (AC) surface course, a 6-in. well-compacted limestone base, a 24-in. sand and gravel subbase, and a 4-CBR buckshot clay subgrade soil. Four-inch WES pressure cells and linear variable differential transducers (LVDT) were installed at various depths in the test section to measure stresses and displacements under various loading conditions. Details of the instrumentation, construction, and testing of the test section are presented in Reference 16.

The meshes of the finite element grid are shown in Figure A1. Since the thickness of the AC surface course was only 3 in., a constant modulus was considered to be appropriate and was used in the computations. Pavement temperature during measurement was about 90°F, and a modulus of 100,000 psi was obtained from Figure 3 at that temperature. Three different computations were made with different stress-strain relations for the granular materials and subgrade soil:

a. Stress-strain relation No. 1.

(1) Granular materials:

$$M_R = K_3 \sigma_3^{K_4} \qquad \text{(bis 3)}$$

and $\nu = 0.3$. For base materials, $K_3 = 13{,}126$ and $K_4 = 0.55$; for subbase materials, $K_3 = 7{,}650$ and $K_4 = 0.59$. (Values are taken from Table 1.)

(2) Subgrade soil:

$$E_t = \left[1 - \frac{R_f(1 - \sin \phi)(\sigma_1 - \sigma_3)}{2C \cos \phi + 2\sigma_3 \sin \phi}\right]^2 E_i \qquad \text{(bis 8)}$$

and $\nu = 0.4$.

b. Stress-strain relation No. 2.

(1) Granular materials:

$$M_R = K_1 \theta^{K_2} \qquad \text{(bis 1)}$$

and $\nu = 0.48$. For base materials, $K_1 = 8300$ and $K_2 = 0.71$; for subbase materials, $K_1 = 2900$ and $K_2 = 0.47$.

(2) Subgrade soil:

Same as in stress-strain relation No. 1.

c. Stress-strain relation No. 3.

(1) Granular materials:

Same as in stress-strain relation No. 2.

(2) Subgrade soil:

$$M_R = K_1 + (K_2 - \sigma_d)K_3 \quad \text{for} \quad \sigma_d < K_2 \qquad \text{(bis 6)}$$

$$M_R = K_1 + (\sigma_d - K_2)K_4 \quad \text{for} \quad \sigma_d > K_2 \qquad \text{(bis 7)}$$

and $\nu = 0.4$.

The reason for selecting large values for Poisson's ratio was explained on page 18. It is believed that large values for Poisson's ratio represent field conditions better than the small value that is used in stress-strain relation No. 1. Both static and resilient moduli for subgrade soil were determined from laboratory tests on undisturbed samples.

Figure A2 compares computed and measured deflections along the load axis of a 30-kip single-wheel load. Using stress-strain relation No. 1, the computed values were much higher than the measured. This was anticipated because of the nature of Equation 3. Equation 3 assumes that the elastic moduli of granular materials depend solely on the minor principle stress σ_3 (confining pressure). When tensile stresses

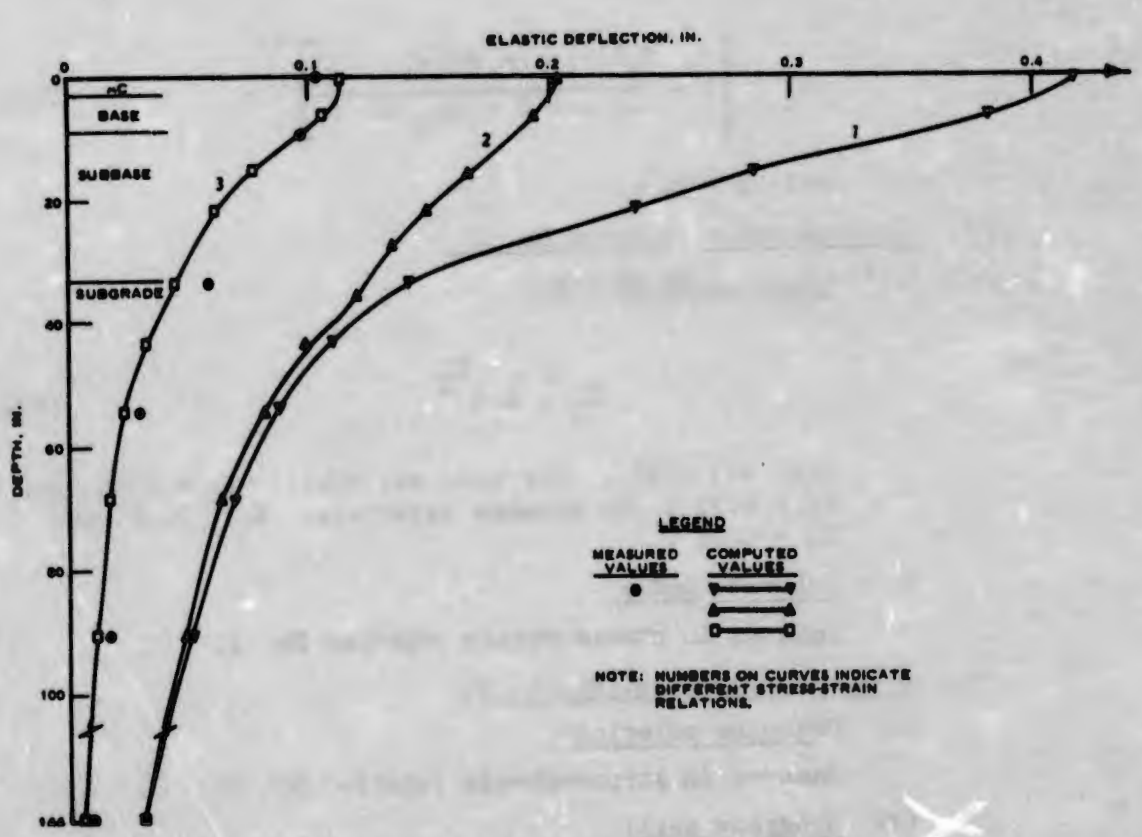

Figure A2. Comparison of the computed and measured deflections along the load axis of a 30-kip single-wheel load

were computed at the bottom of the granular layers, the elastic moduli reduced drastically as the load increment increased, as indicated in the computer outputs. Also, the use of static moduli for the subgrade soil was inadequate because the measured deflections were elastic, i.e., the rebound portion of the curve. Resilient moduli of subgrade soil should be used in the computations, which would result in a reduction of deflections since the resilient moduli are generally much greater than the static ones.

The use of Equation 1 can greatly increase the elastic moduli of granular materials. The major principal stresses σ_1 are generally in compression and are very much greater than the intermediate and minor principal stresses σ_2 and σ_3, which are in tension with load at the bottom of the layers. Hence, in most cases, the first stress invariant θ, the sum of the principal stresses, is positive in magnitude. The

computed deflections based on Equation 1 are shown in curve 2 of Figure A2. The computed deflections, however, were still much greater than the measured. This was also anticipated because static moduli were used in the computations. Nevertheless, it is clearly illustrated that the use of the first stress invariant θ is superior to the use of the minor principal stress σ_3 in characterizing granular materials.

When the static moduli of subgrade soil were replaced by the resilient moduli in the computations, the resulting deflection curve assumed the shape of curve 3 shown in Figure A2. The deflections were greatly reduced and agreed very well with the measured deflections. It is interesting to note that the portion of curve 3 above the subgrade is nearly parallel to curve 2. This is due to the material characterizations for materials above the subgrade soil being the same for these two computations.

Figure A3 compares measured and computed vertical stresses for a

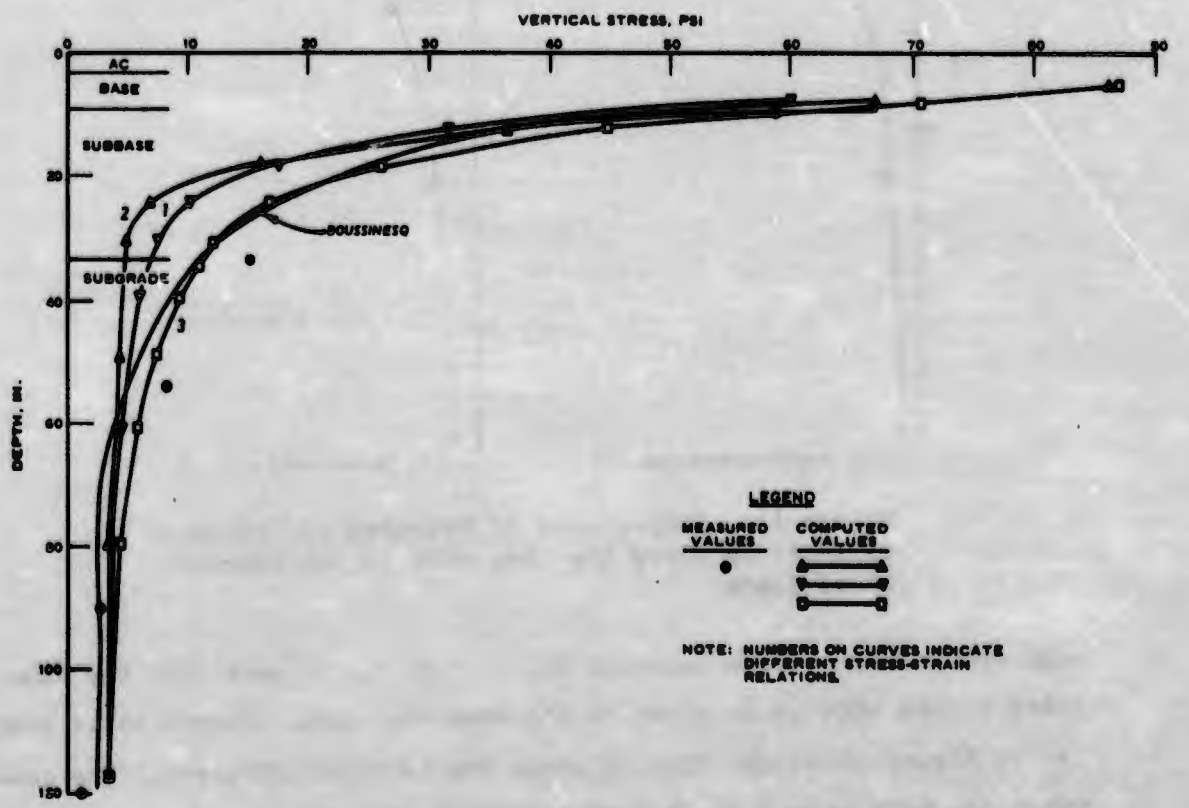

Figure A3. Comparison of measured and computed vertical stresses along the load axis of a 30-kip single-wheel load

30-kip single-wheel load. Curves 1 and 2 were computed with static moduli of the subgrade soil; therefore, the computed stresses at the surface of the subgrade soil were much too low. Since resilient moduli of the subgrade soil were used (providing better subgrade support), the computed vertical stress at the subgrade surface increased and approached the measured value (curve 3). For comparison, the curve for Boussinesq's solution is also presented in Figure A3.

Figure A4 compares measured and computed deflections along the load axes of 15- and 50-kip single-wheel loads. The computations were

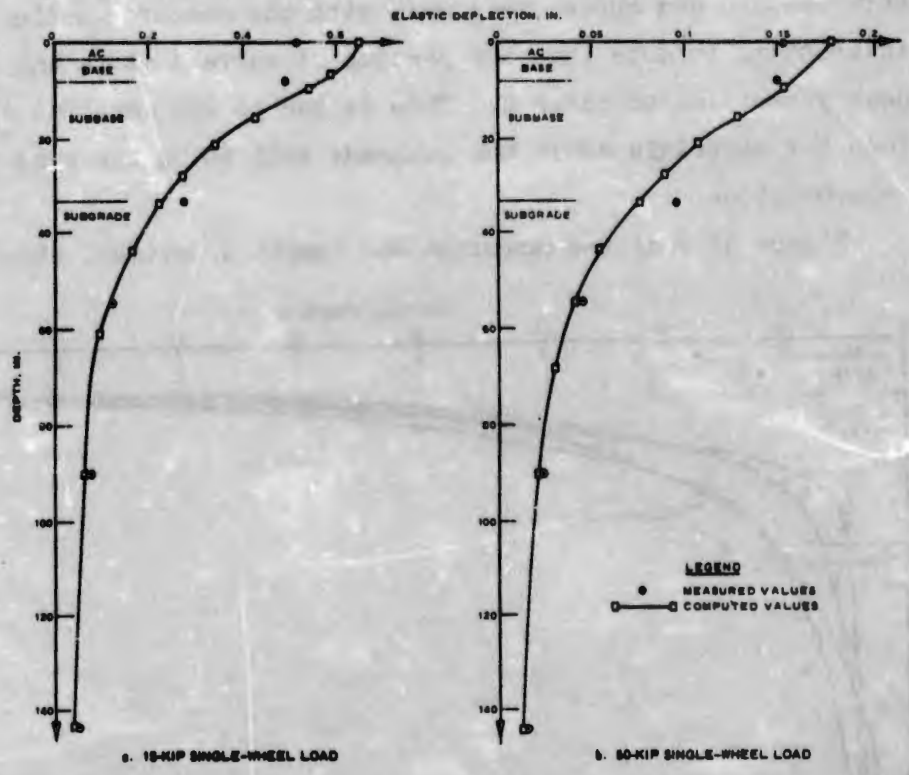

Figure A4. Comparisons of measured and computed deflections along the load axis of two single-wheel loads

made with stress-strain relation No. 3. It can be seen that the computed values were quite close to the measured ones. Figure A5 is similar to Figure A4 except that it shows the vertical stresses. The computations here were also in good agreement with the measurements.

Figure A6 compares measured and computed deflection basins at

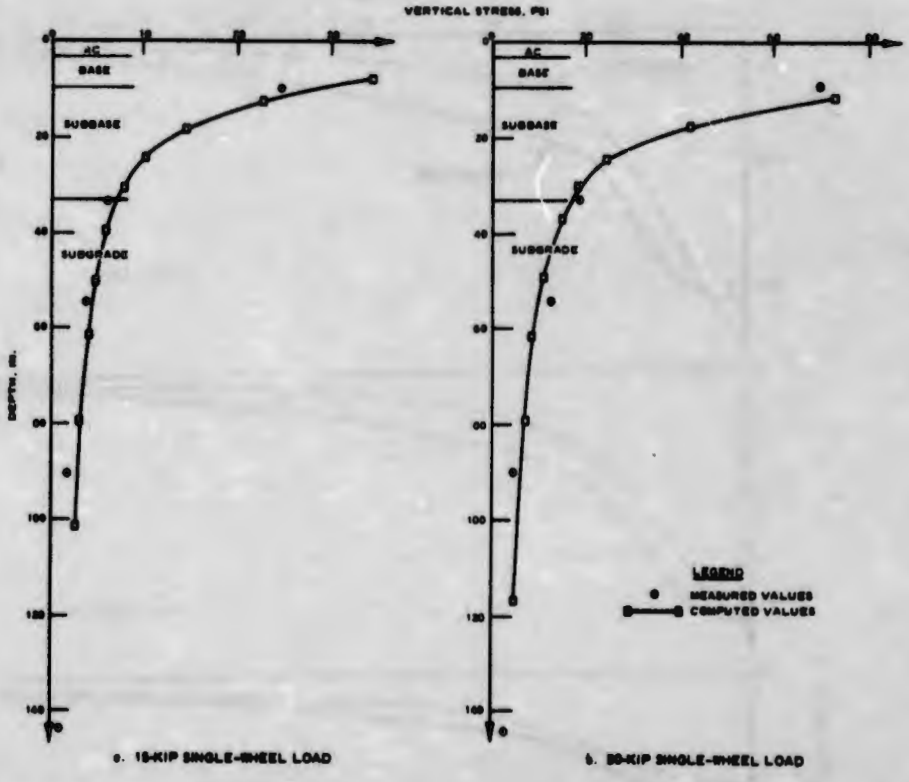

Figure A5. Comparisons of measured and computed vertical stresses along the load axis of two single-wheel loads

various depths under a 30-kip single-wheel load. The computations were made with stress-strain relation No. 3. The agreement between the computations and the measurements along the offset axes was not as good as that along the load axis.

To illustrate the variations of the modulus in the granular materials and the subgrade soil with different stress-strain relations, the moduli in the pavement subjected to a 30-kip single-wheel load are tabulated in Figure A1. Within each element, the first, second, and third values are the moduli corresponding to stress-strain relations No. 1, 2, and 3, respectively. The modulus was not tabulated when tension was developed in an element (a very small positive value was actually assigned to the computer in the computation). It can be seen that the moduli of granular materials increased drastically when the material characterization changed from σ_3-dependent to θ-dependent. When the modulus of the subgrade soil was changed from static to resilient, the

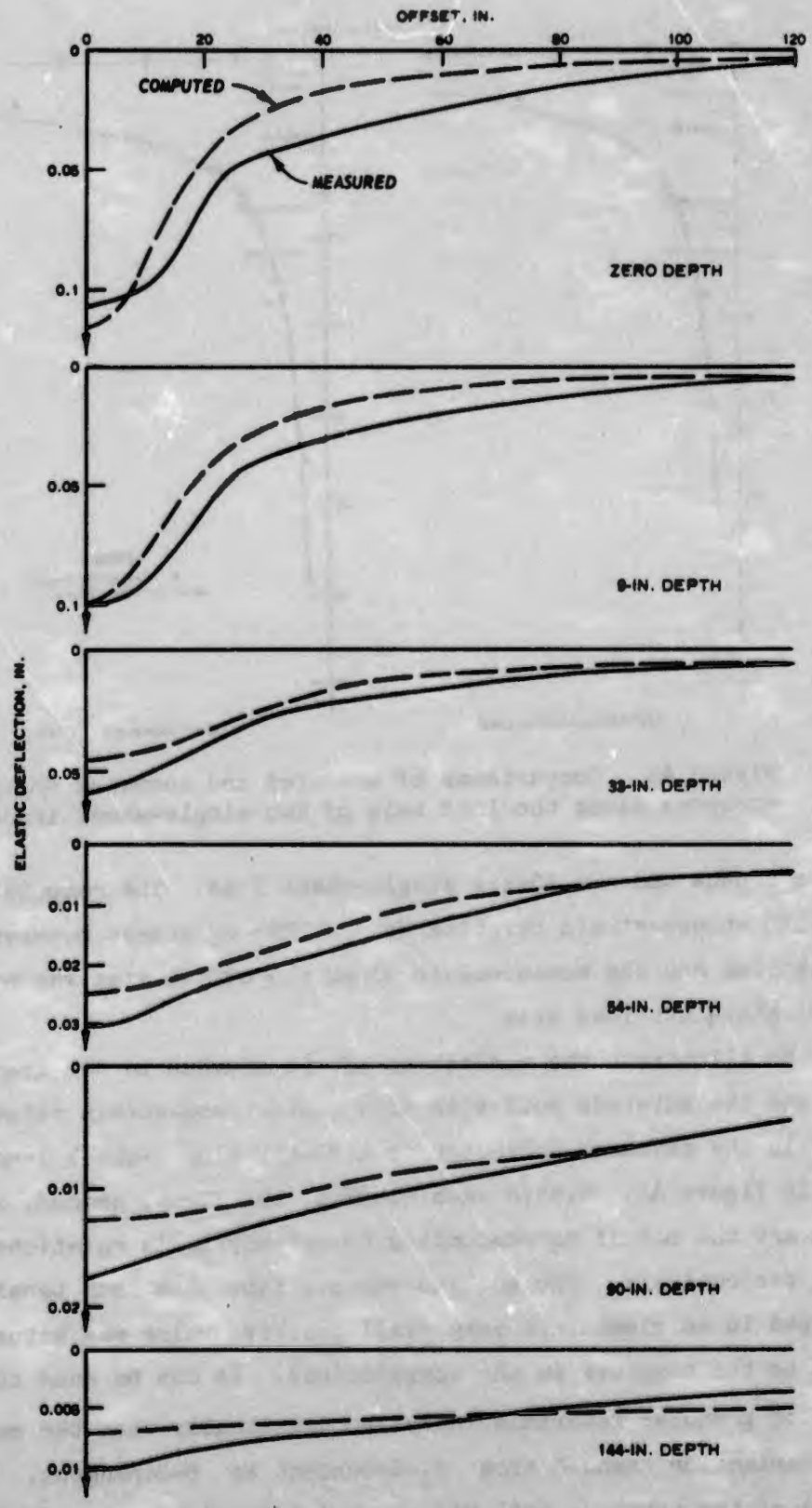

Figure A6. Comparisons of measured and computed deflection basins along the offset axes of a 30-kip single-wheel load

moduli near the bottom of the granular materials around the loaded area increased greatly but increased only slightly elsewhere, while the moduli in the subgrade itself increased significantly.

Figure A7 shows the variation of resilient modulus under different loads. In each element, the first, second, and third values are modulus values under 15-, 30-, and 50-kip loads, respectively. Stress-strain relation No. 3 was used in the computations. In the granular layer, the resilient modulus increased rapidly with an increase in load in the upper portion of the layer around the loaded area where the stress intensities were large, but increased insignificantly elsewhere. This is due to the modulus of granular materials increasing with increasing stress intensity θ, i.e., $\theta = \sigma_x + \sigma_y + \sigma_z = \sigma_1 + \sigma_2 + \sigma_3$. It is interesting to note that in the subgrade soil the resilient modulus decreased with increasing wheel load. This is most significant in the upper portion of the subgrade around the loaded area. Also, the resilient modulus of subgrade soil increased with increasing depth and also increased with offset distances near the subgrade surface. This is in contrast to the granular materials in which the resilient modulus decreased with depth and with offset distances. As shown in Figure 4, the resilient modulus of subgrade soil decreases sharply with increasing deviator stress σ_d and reaches a nearly constant value as the deviator stress further increases. Evidently, the deviator stresses near the subgrade surface around the loaded area were larger than elsewhere in the subgrade and also increased significantly with increasing wheel load.

Figure A8 shows the computed shear and radial stresses in the pavement under a 30-kip single-wheel load; they are shown as the first and second values, respectively, in each element. These computations were also based on stress-strain relation No. 3. Positive numbers denote compression and negative ones denote tension. In this figure, maximum stresses are marked by an asterisk. It can be seen that near the pavement surface the maximum shear stress always occurred near the edge of the load. As the depth increased, the location of maximum shear stress moved outward. For radial stresses, maximum compression occurred at the center of the loaded area near the surface of the AC layer, but tensile

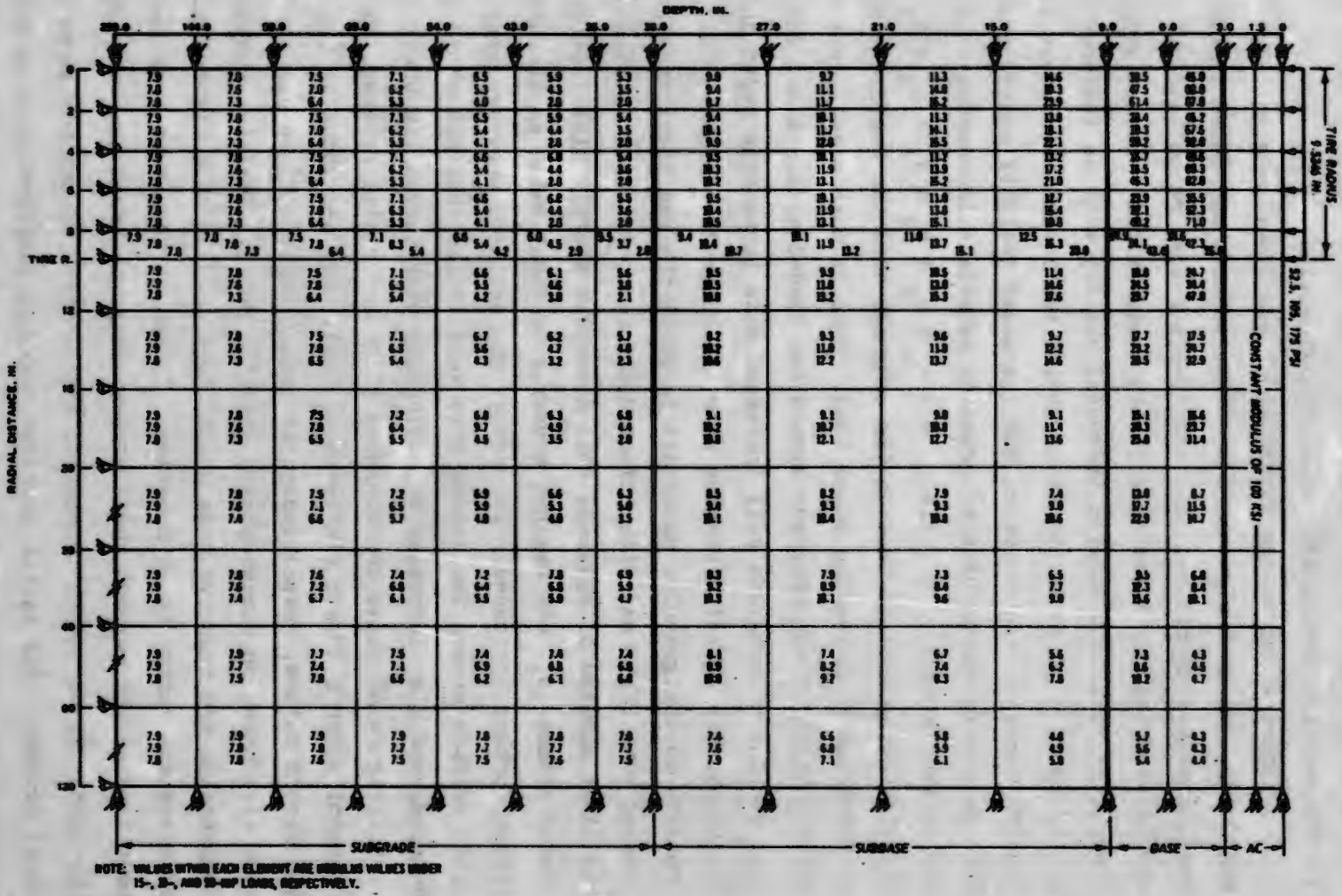

Figure A7. Variations of modulus with single-wheel loads of 15, 30, and 50 kips

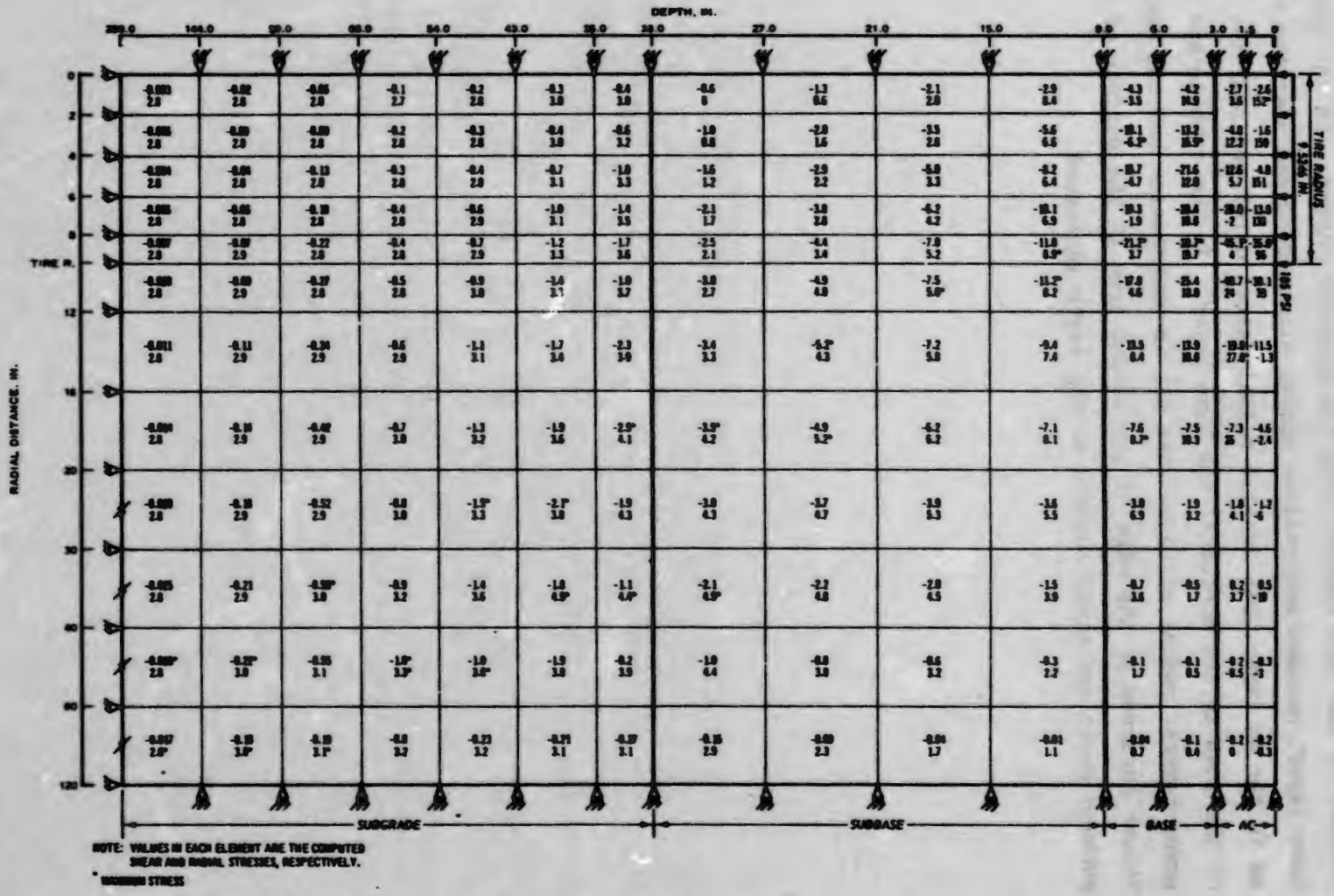

Figure A8. Distributions of shear stresses and radial stresses under a 30-kip single-wheel load

stress did not develop near the bottom of the AC layer. This is possibly because of the firm support from the granular layers. In the granular base layer, maximum compressive radial stress occurred near the center as in the AC layer, but tensile radial stress developed near the center of the load at the bottom of the base layer. In the subbase and subgrade layers, radial stresses were all in compression and the maximum values occurred at the edge of the loaded area at the surface of the subbase layer and moved outward as the depth increased.

REFERENCES

1. Dunlap, W. A., "A Report on a Mathematical Model Describing the Deformation Characteristics of Granular Materials," Technical Report No. 1, Project 2-8-62-27, 1963, Texas Transportation Institute, Texas Tech University, College Station, Tex.

2. Hicks, R. G. and Monismith, C. L., "Factors Influencing the Resilient Response of Granular Materials," Highway Soils Engineering, Highway Research Record No. 345, pp 15-31, 1971, Highway Research Board, National Research Council, National Academy of Sciences, National Academy of Engineering, Washington, D. C.

3. Chou, Y. T. and Ledbetter, R. H., "The Behavior of Flexible Airfield Pavements Under Loads - Theory and Experiments," Technical Report No. AFWL-TR-72-215, Jul 1973, Air Force Weapons Laboratory, Air Force Systems Command, Kirtland Air Force Base, Albuquerque, N. Mex. (Also published as Miscellaneous Paper S-73-66, U. S. Army Engineer Waterways Experiment Station, CE, Vicksburg, Miss.)

4. Kingham, R. I. and Kallas, B. F., "Laboratory Fatigue and Its Relationship to Pavement Performance," Proceedings, Third International Conference on the Structural Design of Asphalt Pavements, 1972, pp 849-865.

5. Coffman, B. S., Kraft, D. C., and Tamayo, J., "A Comparison of Calculated and Measured Deflections for the AASHO Test Road," Proceedings, Association of Asphalt Paving Technologists, Vol 33, Feb 1964, pp 54-91.

6. Hicks, R. G., Factors Influencing the Resilient Properties of Granular Materials, Ph. D. Dissertation, 1970, University of California, Berkeley, Calif.

7. Barker, W. R., Brabston, W. N., and Townsend, F. C., "An Investigation of the Structural Properties of Stabilized Layers in Flexible Pavement Systems," Miscellaneous Paper S-73-69, Table 8, p 43, Oct 1973, U. S. Army Engineer Waterways Experiment Station, CE, Vicksburg, Miss.

8. Seed, H. B., Chen, C. K., and Lee, C. E., "Resilience Characteristics of Subgrade Soils and Their Relation to Fatigue Failures in Asphalt Pavements," Proceedings, First International Conference on the Structural Design of Asphalt Pavements, 1962, pp 611-636.

9. Wang, N. C., Mitchell, J. K., and Monismith, C. L., "Behavior of Stabilized Soils Under Repeated Loading; Stresses and Deflections in Cement-Stabilized Pavements," Contract Report No. 3-145, Report 4, Oct 1970, U. S. Army Engineer Waterways Experiment Station, CE, Vicksburg, Miss.; prepared by University of California under Contract No. DA-22-079-eng-414.

10. Duncan, J. M. and Chang, C. Y., "Nonlinear Analysis of Stress and Strain in Soils," Journal, Soil Mechanics and Foundations Division, American Society of Civil Engineers, Vol 96, No. SM5, Sep 1970, pp 1629-1653.

11. Heukelom, W. and Foster, C. R., "Dynamic Testing of Pavements," Journal, Soil Mechanics and Foundations Division, American Society of Civil Engineers, Vol 86, No. SM1, Feb 1960, pp 1-28.

12. Eringer, A. C., Nonlinear Theory of Continuous Media, McGraw-Hill, New York, 1962.

13. O. J. Porter and Company, Consulting Engineers, "Accelerated Traffic Test at Stockton Airfield, Stockton, California (Stockton Test No. 2)," Report (in 7 vols), May 1948, prepared for U. S. Army Engineer District, Sacramento, CE, Sacramento, Calif.

14. U. S. Army Engineer Waterways Experiment Station, CE, "Investigation of Effects of Traffic with High-Pressure Tires on Asphalt Pavements," Technical Memorandum No. 3-312, May 1950, Vicksburg, Miss.

15. _____, "Flexible Pavements Behavior Studies," Interim Report No. 2, May 1947, Vicksburg, Miss.

16. _____, "Multiple-Wheel Heavy Gear Load Pavement Tests," Technical Report S-71-17, Nov 1971, Vicksburg, Miss.

    Vol I "Basic Report," by R. G. Ahlvin et al.

    Vol II "Design, Construction, and Behavior Under Traffic," by C. D. Burns et al.

    Vol IIIA "Presentation and Initial Analysis of Stress-Strain-Deflection and Vibratory Measurements; Instrumentation," by R. H. Ledbetter et al.

    Vol IIIB "Presentation and Initial Analysis of Stress-Strain-Deflection and Vibratory Measurements; Data and Analysis," by R. H. Ledbetter et al.

    Vol IV "Analysis of Behavior Under Traffic," by G. M. Hammitt et al.

17. _____, "A Limited Study of Effects of Mixed Traffic on Flexible Pavements," Technical Report No. 3-587, Jan 1962, Vicksburg, Miss.

18. Burns, C. D., Ledbetter, R. H., and Grau, R. W., "Study of Behavior of Bituminous-Stabilized Pavement Layers," Miscellaneous Paper S-73-4, Mar 1973, U. S. Army Engineer Waterways Experiment Station, CE, Vicksburg, Miss.

19. Grau, R. W., "Evaluation of Structural Layers in Flexible Pavement," Miscellaenous Paper S-73-26, May 1973, U. S. Army Engineer Waterways Experiment Station, CE, Vicksburg, Miss.

20. Brown, S. F. and Pell, P. S., "A Fundamental Structural Design Procedure for Flexible Pavements," Proceedings, Third International Conference on the Structural Design of Asphalt Pavements, 1972, pp 369-381.

21. Chou, Y. T., "An Iterative Layered Elastic Computer Program for Rational Pavement Design," Report No. FAA-RD-75-226, Feb 1976, Federal Aviation Administration, Washington, D. C. (Also published as Technical Report S-76-3, U. S. Army Engineer Waterways Experiment Station, CE, Vicksburg, Miss.)

22. Ahlvin, R. G., Chou, Y. T., and Hutchinson, R. L., "The Principle of Superposition in Pavement Analysis," Highway Research Record No. 466, 1973.